UNIVERSIDADE DE LISBOA

FACULDADE DE CIÊNCIAS

DEPARTAMENTO DE BIOLOGIA VEGETAL

"GENE DELIVERY TO NEURAL STEM CELLS USING MINICIRCLES AND PLASMIDS WITHOUT CpG MOTIFS"

Mónica Sofia Correia dos Reis

MESTRADO EM BIOLOGIA CELULAR E BIOTECNOLOGIA

2011

UNIVERSIDADE DE LISBOA

FACULDADE DE CIÊNCIAS

DEPARTAMENTO DE BIOLOGIA VEGETAL

"GENE DELIVERY TO NEURAL STEM CELLS USING MINICIRCLES AND PLASMIDS WITHOUT CpG MOTIFS"

Mónica Sofia Correia dos Reis

Dissertação orientada por:

Doutora Teresa Catarina Páscoa Madeira

(Instituto Superior Técnico, Universidade Técnica de Lisboa)

Doutora Susana Maria Serrazina

(Faculdade de Ciências, Universidade de Lisboa)

MESTRADO EM BIOLOGIA CELULAR E BIOTECNOLOGIA

2011

Table of Contents

List of abbreviations

AAV Adeno-associated virus

AD Alzheimer's disease

BDNF Brain-derived neurotrophic factor

BLBP Brain-lipid binding protein

BP Basal progenitors

CNS Central nervous system

CMV Cytomegalovirus

EGF Epidermal growth factor

eGFP *Enhanced* green fluorescent protein

ESC Embryonic stem cells

FGF Fibroblast growth factor

GDNF Glial cell-derived neurotrophic factor

GFAP Glial fibrillary acidic protein

GFP Green fluorescent protein

GLAST Glutamate aspartate transporter

HSC Hematopoietic stem cells

HMB Homemade buffer

iPS induced pluripotent stem cell

MC Minicircles

MC-PP Minicircle Parental plasmid

MSC Mesenchymal stem cells

NEP Neuroepithelial progenitors

NGF Nerve growth factor

NLS Nuclear localization sequence

NP Neural progenitors

NPC Nuclear pore complex

NSC Neural stem cells

PCR Polimerase chain reaction

PD Parkinson's disease

PDGFα Platelet-derived growth factor

RB Resuspension Buffer

RG Radial glia

RT-PCR Real time Polimerase chain reaction

S/MAR Scaffold matrix attachment region

SCI Spinal cord injury

Shh Sonic hedgehog

SVZ Subventricular zone

SGZ Subgranular zone

TLR9 Toll-like receptor 9

VZ Ventricular zone

Acknowledgments

"Our treasure lies in the beehive of our knowledge. We are perpetually on the way thither, being by nature winged insects and honey gathers of the mind"

Friedrich Nietzsche

I want to express my truly gratitude to everyone who followed me during the Master Thesis year, especially to:

Professor Joaquim Cabral, for replying to my e-mail and giving me the opportunity to develop my Master Thesis at the Institute for Biotechnology and Bioengineering (IBB) at Instituto Superior Técnico (IST).

Catarina Madeira, for supervising and supporting me. For believing and trusting my work and for stimulating my scientific interest and perception. You were, without a doubt, the best supervisor I could have, and I leave the laboratory knowing that I gained not only a mentor but also a friend. Thank you for everything!

Carlos Rodrigues, for teaching me how to culture the cells and for all the useful advices.

Filipa Ferreira for accompanying me.

My family, especially my parents and brother, for your support and love. It was for all of you that I wanted to pursue my goals and dreams.

My special friends, for all the given support and friendship.

Abstract

Neural Stem Cells (NSC) are multipotent stem cells, capable of proliferating and differentiating *in vivo* and *in vitro* into astrocytes, oligodendrocytes and neurons. For this reason they hold a great potential for the development of gene and regenerative therapies for the treatment of neurodegenerative diseases and brain cancer. However, transfection of NSCs has proven to be difficult through conventional methods, and the disadvantages associated with the use of viral vectors make non-viral vectors more suitable for the development of gene delivery assays to NSCs. Apart from the non-viral method, one of the most important factors in gene delivery is the type of used vector. One of the factors that mostly affect the vector efficiency is the presence of CpG motifs. These motifs are responsible for the triggering of innate and acquired immune responses contributing to episomal silencing of the transgene. In this study, gene delivery to NSCs was optimized for the use of microporation technology and transfection efficiency was compared for the use of different transfection vectors with low vs. high CpG content, namely, minicircles, pCMV-GFP and pVAX-eGFP.

The optimization of microporation conditions revealed that depending on the electroporation buffer, high number of transfected cells (60 to 75%) and low cell mortality (15-10%) are obtained when using 1500V, 20 ms and 1 pulse or 1800V, 20 ms and 1 pulse as microporation conditions. When comparing the transfection efficiency using different vectors it was evident that Minicircle was the vector that allowed the obtainment of sustained and higher number of transfected cells (75%) without affecting their survival (80-90% of cell viability) and morphology. The quantification of vector copies in the nuclei revealed that the optimal dose to transfect NSCs is around 0.8 µg, and that, although a similar number of Minicircle and pCMV-GFP copies per nucleus is found, the first are the vectors that yield the highest expression levels. Long term analysis also showed Minicircles are less degraded, exhibiting higher number of copies and GFP expression than pCMV-GFP or pVAX-eGFP. Finally, microporation did not seem to affect NSCs differentiation potential.

Taken together, these results offer the first insights in the use of microporation and minicircles in non-viral transfection of NSCs, suggesting that microporation is a promising tool for NSCs transfection and that minicircles offer a new model of efficient and safe non-viral gene delivery to NSCs and have unquestionably a potential use for clinical applications and genetic engineering.

Keywords: CpG motifs; Microporatio; Minicircles; Neural stem cells; Non-viral gene delivery; plasmid DNA;

Resumo

Células estaminais representam um grupo específico de células indiferenciadas que apresentam a capacidade de se auto-renovar e de se diferenciar, quando estimuladas por determinadas condições, em células várias linhagens distintas. Existem dois tipos distintos de células estaminais: embrionárias e adultas. As células embrionárias apresentam a capacidade de se especificarem em vários tipos celulares no entanto, os problemas éticos muitas vezes associados com o seu isolamento e potencial cancerígeno, limitam o seu uso. Por este motivo, o interesse em células estaminais adultas, que apresentam apenas a capacidade de se especificar em tipos celulares provenientes do seu tecido de origem, tem vindo a aumentar exponencialmente.

Células estaminais neurais (Neural stem cells – NSC) representam uma população de células que pode ser isolada a partir de tecido cerebral embrionário, fetal ou adulto. No cérebro em desenvolvimento estas células existem como progenitores neuroepiteliais que se diferenciam em vários progenitores neurais que vão dar origem aos três tipos celulares característicos do sistema nervoso, astrócitos, oligodendrócitos e neurónios. No sistema nervoso adulto, estas células representam uma população de astrócitos que têm a capacidade de se diferenciar em caso de infecção ou inflamação, e habitam nichos específicos na zona subventricular do prosencéfalo e na zona subgranular do hipocampo. A sua capacidade única de se diferenciarem em células do sistema nervoso e de, após enxerto, conseguirem ultrapassar a barreira hematoencefálica, faz com que estas células apresentem um elevado potencial para o desenvolvimento de terapias regenerativas e genéticas para o tratamento de doenças neurodegenerativas e de cancro do cérebro.

Em cultura, estas células são aderentes ou formam complexos esféricos de progenitores neurais, apresentam a forma bipolar e expressam factores característicos de células neuronais, tais como nestina, Sox2 e Pax6, e astrogliais, tais como GFAP, GLAST, BLBP e RC2. A capacidade de diferenciação que estas células apresentam e o desenvolvimento de protocolos de diferenciação simples e eficazes fez com que as NSCs tenham sido alvo de diversos estudos de regeneração de tecidos e transferência de genes. Estudos recentes demonstraram que em caso de enxerto, as NSCs conseguem diferenciar-se em neurónios dopaminérgicos e substituir lesões em modelos de doença de Parkinson e conseguem reduzir o processo inflamatório em modelos de esclerose múltipla. Em termos de entrega de genes, os estudos efectuados demonstraram que as NSCs podem ser transfectadas e entregar genes terapêuticos que potenciam o melhoramento de várias doenças de foro neurológico.

Um dos grandes problemas até agora tem sido o desenvolvimento de métodos de transfecção eficientes. Até muito recentemente, a transfecção de NSCs era basicamente feita através de métodos virais, no entanto os problemas patogénicos associados a estes vectores e a possibilidade de indução de mutagénese das células transfectadas fez com que a atenção dos cientistas divergisse para as metodologias não virais. Em comparação com as primeiras, estas metodologias oferecem uma série de vantagens, tais como, maior capacidade de empacotamento, menor imunogenicidade, fácil e maior segurança de manuseamento. A entrega de genes usando estes métodos pode ser feita através de tratamentos químicos, como partículas de fosfato de cálcio, biopolímeros biodegradáveis e liposomas catiónicos, e através de tratamentos físicos, tais como sonoporação, bombardeamento de partículas, magnetofecção, electroporação e microporação. Para além do método de transfecção, há que ter em atenção o tipo de vector usado. Após transfecção, os vectores têm que ultrapassar barreiras extra e intracelulares que causam silenciamento episomal do transgene. É por este motivo que têm sido desenvolvidos muitos trabalhos com o intuito de melhorar os vectores. Um dos factores que mais afecta a eficiência de um plasmídeo é o conteúdo deste em motivos CpG. Estes dinucleótidos não-metilados são característicos de genomas bacterianos e, se presentes em plasmídos, são reconhecidos pelo sistema imunitário de mamíferos, mais especificamente por células que expressam TLR9, despoletando reacções imunológicas inatas e secundárias que levam à degradação do vector e posterior silenciamento do transgene. Recentemente têm sido produzidos plasmídeos de conteúdo reduzido em motivos CpG que em relação aos pDNAs convencionais, apresentam eficiência e persistência melhoradas. Para além destes tipos de vectores, o desenvolvimento da tecnologia de minicirculos, que são pequenos vectores desprovidos de sequências bacterianas e de conteúdo CpG reduzido, permitiu um melhoramento de 10 a 10,000x das eficiências de transfecção em relação aos pDNAs convencionais. O objectivo principal deste estudo foi a optimização das condições de transfecção não viral de NSCs (CGR8-NSC) por microporação e a comparação das eficiencias de transfecção de NSCs quando transfectadas com minicirculos e pDNAs com conteúdo em motivos CpG reduzido ou mesmo inexistente.

Neste estudo, foram feitas duas optimizações das condições de microporação para o uso de dois tampões de electroporação diferentes, o RB, um tampão de formulação desconhecida, e o HMB, um tampão preparado no laboratório e que já tinha sido utilizado para transfectar células HEK293T e células estaminais mesenquimatosas. A microporação com o tampão RB foi feita transfectando pVAX-eGFP e variando a voltagem (entre 1400 e 1600V), a duração do pulso (20 e 30 ms) e o número de pulsos (1 e 2). A condição que no geral demonstrou ser mais eficaz foi 1500V, 20 ms e 1 pulso (percentagem de células

transfectadas ≈ 60%; viabilidade e recuperação celular 85-90%). A optimização com HMB foi feita microporando as NSCs com dois vectores diferentes (pVAX-eGFP e MC-GFP) e variando a voltagem entre 1600 e 1900V. Apesar de, com o aumento da voltagem se ter verificado, em ambos os casos, uma diminuição das viabilidades e recuperações celulares (mais acentuada em células transfectadas com pVAX-eGFP), no geral, a condição que obteve os melhores resultados, exibindo as percentagens de células transfectadas (50 e 75% com pVAX-eGFP e PC-GFP) e rendimentos de transfecção (47 e 69% com pVAX-eGFP e MC-GFP) mais elevadas foi 1800V, 20 ms e 1 pulso. Um outro ensaio de optimização foi efectuado para determinar a quantidade ideal de DNA para transfectar NSCs. Para isto, NSCs foram ressuspendidas em RB e transfectadas com várias quantidades de pVAx-eGFP (0.5, 0.8, 1.0 e 1.5 µg) usando 1500V, 20 ms e 1 pulso como condições de microporação. Apesar de o aumento de DNA não ter afectado a percentagem de células GFP^+ (≈50%) e de ter provocado uma diminuição das viabilidades e recuperações celulares, 0.8 µg foi a quantidade de pDNA que exibiu o maior rendimento de transfecção (≈40%), tendo sido por isso considerada a quantidade ideal de vector para transfectar NSCs.

Para testar a eficiência de transfecção de minicirculos e outros pDNAs com conteúdo reduzido ou inexistente em CpGs as NSCs foram transfectadas com 2.0×10^{11} moléculas de cada vector. A transfecção com plasmídeos sem motivos CpG (pCpGfree-eGFP) revelou-se muito aquém do esperado, e quando comparando com NSCs transfectadas com pVAX-eGFP, a percentagem de células GFP^+ era menor e o decaimento da expressão do transgene ao longo do tempo mais rápido em células transfectadas com pCpG-eGFP, indicando que talvez, o promotor deste plasmídeo não seja tão eficiente como o do pVAX-eGFP. Comparando células transfectadas com minicirculos (MC-GFP) com outros pDNAs (pCMV-GFP – plasmídeo correspondente de MC-GFP, e pVAX-eGFP) verificou-se que usando MC-GFP é possível manter elevados níveis de células transfectadas (≈75%) sem comprometer a viabilidade celular (80-90%) e a morfologia bipolar característica das NSCs em cultura. Adicionalmente, a expressão do gene mantém-se mais alta com MC-GFP ao longo de 10 dias e não afecta a proliferação celular.

Testes adicionais foram efectuados para quantificar o número de cópias de vector no núcleo de NSCs transfectadas. Em estudos anteriores tinha-se verificado que há uma certa dose de plasmídeo a partir do qual a expressão do transgene satura. Em NSCs verificou-se que, independente do vector, a partir de 0.8 µg há uma estabilização e posterior decaimento da expressão da GFP, e, quando comparando o número de cópias de cada vector no núcleo, verificou-se que apesar da quantidade de MC-GFP e pCMV-GFP ser semelhante, o nível de expressão do primeiro era mais elevado. Adicionalmente, a análise ao longo de 10 dias da quantidade de cópias do núcleo revelou que o MC-GFP era o vector que se

encontrava em maior quantidade no núcleo e o que revelava maiores níveis de expressão do transgene, indicando que este, devido ao seu menor tamanho e conteúdo CpG mais reduzido (≈6%) é menos degradado que os outros plasmídeos. Em comparação, os resultados com pCMV-GFP e pVAX-eGFP, que apresentam conteúdo semelhante em motivos CpG (≈7%), diferem muito entre si, apresentando o pCMV-GFP eficiências e viabilidades celulares mais elevadas. Este facto é difícil de ser explicado mas há três diferenças entre estes dois plasmideos que podem justificar esses valores: i) diferente sinal de poliadenilação dos dois plasmídeos (pVAX-eGFP apresenta o sinal BGH e o pCMV-GFP apresenta o sinal SV40), que como estudos anteriores já demonstraram pode influenciar os níveis de expressão, ii) diferenças na sequência do gene reporter que pode originar uma proteína com maior ou menor intensidade de fluorescência; iii) ou ao nível de purificação de cada plasmídeo. Finalmente, nem o uso de microporação nem a transfecção com plasmídeo afectou a capacidade de diferenciação das NSCs em neurónios.

Comparando os resultados obtidos é possível concluir que o uso de microporação como método de transfecção de NSCs dá origem a elevadas eficiências de transfecção. Em comparação com os outros pDNAs, os Minicirculos foram os vectores que demonstraram as melhores eficiências de transfecção e os maiores níveis de expressão do transgene sem comprometer a morfologia e a viabilidade das células. Pode-se concluir que o tamanho destes vectores e que a diferença e 1% no conteúdo em motivos CpG é suficiente para que o silenciamento episomal do transgene seja mais fraco com MC-GFP. Como trabalho futuro, seria interessante avaliar a expressão de TLR9 em NSCs após transfecção para verificar se há realmente silenciamento devido aos motivos CpG e quantificar o RNA mensageiro para avaliar a estabilidade e frequência do transgene. Seria também muito benéfico avaliar a eficiência dos minicirculos através de transfecção por outros métodos não virais, tais como, lipofecção ou magnetofecção, e efectuar estudos *in vivo* para avaliar o tráfico intracelular de minicirculos, e também clonar um gene de interesse nos minicirculos para avaliar o seu potencial no desenvolvimento de futuras terapias para doenças de foro neurológico.

Até à data, ainda não tinham sido efectuados estudos de transfecção em NSCs usando microporação ou minicirculos. Este trabalho representa a primeira perspectiva para o uso destas tecnologias para a transfecção destas células e indica que os minicirculos representam um novo modelo eficiente e seguro de entrega não viral de genes para NSCs e uma alternativa muito promissora para o desenvolvimento de terapias para o tratamento de doenças neurodegenerativas ou cancro do cérebro onde uma expressão transiente de transgene pode ser necessária.

Palavras-Chave: Células estaminais neurais; DNA plasmídico; Entrega de genes não-viral; Microporação; Minicirculos; Motivos CpG.

1. Introduction

1.1. Stem cells

A stem cell is a specific type of cell that has the potential to differentiate into one or more specialized cell type and the unique capacity of self-renewal for an expanded period of time. Unlike the majority of cells which are committed to conduct a specific function, a stem cell maintains an unspecialized state until it receives signals to differentiate into a tissue- or organ-specific cell kind [2]. Due to their special proliferative capacity and high plasticity, these cells represent an invaluable tool to basic research and an incredible resource for the repair and regeneration of diseased or damaged cells and tissue [3].

Stem cells can be found since the early stage of the embryo until the end of life and can be categorized as embryonic or adult, depending on their tissue of origin. Embryonic stem cells are derived from the inner cell mass of the blastocyst (4 to 5- day embryo) and possess the remarkable property of pluripotency, giving rise to a wide variety of cell types representative of the three primary germ layers in the embryo (mesoderm, endoderm and ectoderm) [3-4]. For this reason, they hold a great promise for tissue engineering and cell replacement therapies, however, their potential use in biomedical treatments is still controversial due to ethical concerns related to their isolation and because of their tumorigenic potential [5].

Adult stem cells are lineage-restricted undifferentiated cells, i.e. multipotent cells, with the capacity of giving rise to progeny cells of their correspondent tissue of origin [6]. These tissue-specific cells are scarce and present in a metabolically quiescent state in specialized tissues, such as the brain, bone marrow, liver, skin and gastrointestinal tract. Nowadays, on account of their high accessibility and minimally invasive harvesting procedures, there is a rising interest in these cells. The best known example of adult stem cell is the Hematopoietic stem cell (HSC) which can be isolated from the bone marrow niche and has the capacity to originate all blood cell types. Mesenchymal stem cells (MSC) and Neural stem cells (NSC) are other good examples of well studied adult multipotent cells. MSC have the potential to differentiate into different mesodermal cell lineages and are present in almost all tissues, however for therapeutic applications they are preferably isolated from the bone marrow and the umbilical cord blood [7]. NSC can be isolated from embryonic, fetal or adult brain tissue and are capable of generating neurons and glia in the developing brain. In the mammalian adult brain NSCs exist in niches that support symmetric self-renewal and fate-committed asymmetrical divisions that potentiate de replacement and recovery of lost neural cells [8].

1.2. Sources of Neural Stem Cells

1.2.1. Embryonic neurogenesis

The main features of Neural Stem cells (NSCs) reside in their ability to self-renewal, proliferate and generate multiple cellular lineages, such as neurons, astrocytes and oligodendrocytes both *in vivo* and *in vitro.* Their morphological and phenotypic identities vary depending on the developmental stage and region occupied by these cells during adult life. In the early embryonic stage, predetermined programs give rise to spatiotemporally different NSC populations in a process called Neurogenesis. This process begins with the induction of the neuroectoderm, which forms the neural plate that folds to originate the neural tube. In the embryonic neural tube, NSCs exist as neuroepithelial stem cells that undergo differentiation into distinct neural progenitors and posterior specification into neuronal lineages through asymmetrical cell divisions in the germinal ventricular zone (VZ). After the neurogenic phase NSCs acquire gliogenic competence and start differentiating into glia in the subventrivular zone (SVZ). This process leads to the specification of astrocytes and the disappearance of the VZ. After brain development, some parts of the brain still harbor sites where adult neurogenesis remains active with the sole purpose of maintaining homeostasis of the central nervous system (CNS) [9].

1.2.2. Neural differentiation of embryonic stem cells

The understanding of the processes involved in embryonic neurogenesis and the progress in cell culture methodologies enabled the development of protocols that induce neuralization of ESCs *in vitro*. The overall advantage of ESC derived NSCs is that these cells retain a developmental competence to patterning signals giving rise to regional subtypes that can be transplanted *in vivo* and differentiate into functional neuronal entities. Early ESC neuralization attempts reported that, in minimal inductive conditions [10], ESCs were capable of differentiating into progressive neural progenitors that expressed distinct neural markers [11], however, the resulting cultures had a heterogeneous profile characterized by the coexistence of undifferentiated ESCs and different neural progenitors. Therefore, new protocols, based on the production of embryoid bodies [12], or stromal feeder co-cultures [13] were developed. Under these conditions, the originated cell populations exhibited uniform biochemical and electrophysiological characteristics. Nowadays, with the increasing comprehension of the developmental and functional mechanisms of ESC derived neurons, more effective procedures are being established. Recently, Chambers and colleagues, based on the understanding of the involvement of the SMAD signaling pathway in neural induction, developed a new protocol in which a dual-SMAD inhibition, by the synergistic action of Noggin and SB431542, induced rapid and complete neural conversion

of human ESCs [14]. Apart from ESCs, induced pluripotent stem cells (iPS) represent another great source of cells for differentiation into NSCs. Many protocols for neuralization of iPS are being developed and they provide a unique opportunity for the development of autologous therapies and tissue replacement [15].

1.2.3. Adult neural stem cells

Adult Neural Stem Cells (aNSCs) are present in specific niches in the subventricular zone (SVZ) and subgranular zone (SGZ) of the adult brain where they undergo adult neurogenesis. In these areas, their regulation is managed by fate—controlling molecules and signaling pathways. These molecules are members of the fibroblast and epidermal growth factor families and permit the expansion and specialization of adult neural progenitors *in vivo* and *in vitro*. Some of the most studied mediators are: epidermal growth factor (EGF) [16] and platelet-derived growth factor (PDGF-α) [17], that induce gliogenic specification, and fibroblast growth factor (FGF) [18], Sonic hedgehog (Shh) [19] and brain-derived neurotrophic factor (BDNF) [20] that are responsible for the differentiation into neuronal cells. *In vivo*, neurogenesis is regulated by the action of immune effector cells called microglia that are abundantly present in the adult CNS. During an injury, microglia secretes neurotrophic and neurogenic factors that potentiate the recovery of the damaged regions and increase the neurogenic process [21-22].

The most active zone of adult neurogenesis is the SVZ of the forebrain. This area contains a subpopulation of astrocytes that function as aNSCs *in vivo* and are known as Type-B cells, which in turn, can be subdivided in Type B1 and B2 cells. Type-B1 cells are considered true aNSC and are in contact with the ventricular cavity where, in response to vascular signals, differentiate into neural progenitors (Type C cells). These progenitors undertake symmetrical divisions and give rise to neuroblasts (Type A cells) that migrate through the rostral migratory stream, aided by Type B1 and B2 cells, to the olfactory bulb where they specify as interneurons. In the SGZ in the dentate gyrus of the hippocampus, neuronal progenitors (Type-B cells) differentiate into granular neurons. However, these neuronal progenitors have a limited capacity of specification. They suffer asymmetrical divisions that instigate a regionally determined differentiation into granular neurons that act as regenerative entities in the brain [23].

1.3. Characterization of NSCs

1.3.1. *In vitro* proliferation of NSCs

NSCs can be proliferated as Neurospheres or in adherent conditions. After isolation NSCs are plated in low attachment tissue culture plastic dishes in serum-free media supplemented with the mitogens EGF and FGF [24]. Under these conditions cells that are undergoing specification die and NSCs form free-floating aggregates. The Neurosphere system is thought to provide a three dimensional environment that mimics neurogenic niches [25], however long-term cultures of neural progenitors as aggregates are difficult to maintain due to the occurrence of changes in the differentiation and self-renewal capacities, and the incidence of chromosomal instability [26-27].

In the first approaches, the adherent system involved, , expansion of NSCs on biopolymer-coated dishes in serum-free conditions [28]. These procedures permitted the exploration of NSCs multipotentiality but the cultures were short-termed and did not allow an efficient immortalization. Nowadays adherent propagation of NSCs is performed under the action of EFG and FGF-2 [29], or, as recent data show, under exposure to angiogenic factors [30]. In these conditions, cells undertake symmetrical divisions, maintain an undifferentiated state for a long period of time and retain their tripotential differentiation capacity.

1.3.2. *In vitro* differentiation of NSCs

Due to the potential that NSCs have to differentiate into neurons, astrocytes and oligodendrocytes, a number of protocols have been developed for controlled *in vitro* specification in one of the three possible fates. Differentiation within neurospheres is achieved by mitogen removal after attachment onto substrate coated coverslips [29]. Under these conditions NSCs form primary neurospheres and specify into neuronal progenitors. Upon replating the neural progenitors give rise to secondary aggregates where they differentiate into GABAergic interneurons, astrocytes and oligodendrocytes, however, with the posterior passages, the maintenance of neurogenic competence declines and the yield of gliogenesis increases thus originating an uncontrolled pattern of differentiation. In the monolayer adherent system, NSCs give rise to antigenically and electrophysiologically mature neurons, oligodencrocytes and astrocytes after prolonged expansion under optimized differentiating conditions [29, 31-32]. These *in vitro* differentiated cells can be efficiently transplanted into the brain and establish synaptic connection with the cells of the nervous system [33].

1.3.3. *In vivo* and *In vitro* phenotype of NSCs

There are currently four types of known phenotypically distinct NSCs: Neuroepithelial progenitors (NEP), Radial Glia (RG), Basal Progenitors (BPs) and Adult neural stem cells (aNSCs).

NEPs are present during the embryonic development of the CNS and express nestin, Sox1, Sox2 and Pax6, markers for immature neural cells, and some ESC markers, such as Oct4. The expression of nestin, Sox2 and Pax6 persists throughout the specification of primitive NEPs into the subsequent neural progenitors and is essential to the neurogenic process [34-36]. *In vitro*, these primitive NSCs lose the expression of ESC markers with the passages and become more committed to specify into neural progenitors. At the beginning of neurogenesis, NEPs give rise to RGs that serve as the main progenitors in the developing brain. RGs express astroglial markers, such as astrocyte specific glutamate aspartate transporter (GLAST), glial fibrillary acidic protein (GFAP), brain-lipid binding protein (BLBP) and RC2, and neurogenic markers like nestin, Sox2 and Pax6. Recent findings suggest that RGs can also be found in a non-ventricular niche in the adult spinal cord of mice (SCRGs) and are phenotypically similar to adult NSCs of the SVZ [37].

In the adult brain, BPs potentiate the production of neurons, however, their propagation *in vitro* is difficult so little is still known about them. Adult NSCs are the main progenitors of adult neurogenesis and combine the expression of radial glial markers, like GFAP, GLAST, BLBP and RC2; neural precursor markers like, nestin, Sox2 and Pax6; regional markers like Otx2 and Hoxb9 and others like Musashi 1 and CD133 that maintain their stemness. *In vitro*, aNSCs are antigenically similar to neurogenic RGs in the brain when grown in adherent conditions; however, when propagated as neurospheres, their phenotype is characterized by the presence of differentiated cells in the sphere core surrounded by RG-like neural progenitors [8, 26, 32].

1.4. Therapeutical applications of NSCs

In recent years, the successful production of neurons and glia from stem cells in culture fuelled efforts to develop stem-cell-based transplantation therapies for neurological disorders. It is well known that within the CNS, endogenous neural progenitors support its 'self-repair' during inflammatory disorders, such as spinal cord injury and stroke [38-39]. Although efficient, endogenous stem cells are not able to promote full and irreversible repair of the CNS. Adult neurogenesis is highly influenced by the surrounding microenvironment, and, upon inflammation, the supporting cells secrete molecules that attract inflammatory cells. NSCs can perceive these changes as dysfunctions and induce an uncontrolled neurogenic process [40].

Nowadays, many laboratories are diverting their attention to the development of therapies for many CNS disorders, such as, Parkinson's disease, Huntington's disease, multiple sclerosis, stroke, traumatic brain injury, Alzheimer's disease, epilepsy, and others. These diseases are characterized by progressive neuronal degeneration that can ultimately be fatal. Stem-cell based approaches for these diseases involve the engraftment of *in vitro* propagated NSCs or differentiated neuronal cells for the restoration of a lost function. When transplanted they have low immunogenicity, are able to migrate and overcome the blood-brain barrier, and upon transfection, allow vector-directed differentiation or drug delivery [41]. Many studies have documented that neural progenitors, for instance, can be efficiently engrafted to Parkinson's disease models, migrate to the injured areas and specify into dopamine neurons [42], can survive, migrate and differentiate under the influence of the surrounding microenvironment in stroke models [43] or can reduce brain inflammatory process in multiple sclerosis models [44].

NSCs can also be used as drug delivery vehicles. They can be transfected and produce specific neurotrophic or neuroprotective factors that promote a long-lasting amelioration and regression of the symptoms of neuronal disorders. A few authors have published results regarding, for example, the delivery of GDNF engineered NSCs to PD and amyotrophic lateral sclerosis models [45-46], the delivery of NGF or BDNF to AD models [47-48], or the delivery of VEGF to promote recovery in SCI models [49-50]. NSC based gene therapy also represents a promising tool for the treatment of brain tumors by the delivery of molecular agents that promote the conversion of prodrugs into anticancer substances, and immunostimulating cytokines [51].

1.5. Gene delivery to NSCs

1.5.1. Viral methods

Lately, many efforts have been made to improve the transfection efficiency of NSCs in order to provide better opportunities for future therapeutic applications. Viruses like retrovirus and lentivirus integrate into the host genome and allow stable gene transfer and long-lasting expression. In contrast, adenovirus and adeno-associated virus (AAV) are non-integrating particles that cause no side effects in humans, and allow transient expression of the transgene [52]. Although efficient, there are still some drawbacks related to their use. These vectors have limited transgene capacity, trigger cytotoxic and immunogenic reactions, cause mutagenesis due to their random integration in the host genome [52-53], and in NSCs they affect differentiation and block neurogenesis [54]. At present, a special attention is being given to AAV vectors. These vectors were initially considered nonintegrative and nonpathological however, it has been demonstrated that they integrate into the host genome and trigger malignant transformation of the cells [55-56]. Nevertheless, some of the newest methodologies for gene delivery take advantage of their demonstrated capacity and available capsid libraries to design new hybrid vectors that consist of AAV packaged plasmids [57].

1.5.2. Non-Viral methods

Regardless of having lower transfection efficiencies and low cell viabilities, there's an increasing interest in non-viral gene delivery methods. When compared to viral methods, non-viral methods are cheaper, easier to manage, have a wider range of putative cell targets, lower immunogenicity, lesser toxicity, bigger packaging capacity and allow transient expression, a feature that might be beneficial for therapeutic strategies where a short duration of transgene expression is necessary [58]. These methods are used to transfect different molecules, such as, RNAs (e.g. siRNAs), proteins (e.g. antibodies) and DNA which is mostly delivered as plasmid vectors (pDNA) that have been cloned to contain a transgene expression cassette [59], and rely on a physical treatment or on chemical or biological particles that are used as carriers.

Some of the most used chemical DNA delivery methods are:

- Calcium phosphate-mediated transfection which involves incubation of the cells with calcium phosphate coated pDNA. This method is very efficient yet restricted to some cells and sensitive to the amount of input pDNA [60].
- Biodegradable cationic polymers that are used for the controlled release of DNA into the cell or tissue of interest. These polymers have a reduced toxicity and avoid polymer accumulation in the cells, however, their slow degradation rate and the inefficient

membrane destabilizing peptides available influence the effectiveness of these structures [61]

- Cationic liposomes which are vesicular structures of positively charged lipids that once surrounding DNA form lipoplexes. These systems have a low toxicity *in vitro*, but can exhibit some toxicity and low transfection efficiencies *in vivo* due to the physiochemical properties of the cationic lipid/DNA complexes [62].

The most popular physical DNA delivery systems are:

- Sonoporation that consists on the permeabilization of the cell membrane through exposure to low-field ultrasounds that induce the uptake of large molecules into the cell. This technique is used in targeted gene transfer both *in vivo* and *in vitro*, however, extended exposure to low-field ultrasounds results in increased cell mortality, thus the procedure needs to be carefully applied [62]; Gene gun which is based on the precipitation of DNA on small particles of a heavy metal, usually gold, and posterior injection, using a pistol. At present there are many listed gene gun clinical trials for Hepatitis B, malaria and influenza yet, this method is only applicable on superficial tissues (e.g. skin) due to the high level of cell damage caused by the velocity of the particles [62];
- Magnetofection that involves the association of the DNA with magnetic nanoparticles which are transferred to the cells by the application of a magnetic field. Although promising, the use of magnetofection *in vivo* is still limited due to the inaccessibility of the targeted tissues to magnetic field and hydrodynamic forces. Ongoing improvements of this procedure involve, in some cases, the combination of the magnetic complexes with cationic lipids [62-63];
- Electroporation, which is a powerful tool that relies on the application of a short electric pulse that leads to a permeable state of the cell membrane so that the molecules can be driven into the cell through elecrophoretic and electro-osmotic forces. This technique is used to transfer molecules of different sizes (e.g. genes, proteins, ionic dyes and drugs) into the cell, however, there are still some problems needing to be solved such as low viabilities and transfections caused the massive cell mortality triggered by the electric pulse [62]; To overcome some of the problems associated with electroporation, a new technology called Microporation was developed. This new layout provides high transfection efficiencies and cell viabilities and is based on the use of a pipette tip as electroporation area and a capillary electrode which allows maintenance of pH and temperature, minimizes turbulence and avoids ion metal generation [64]. Recent studies have proven that microporation is an easy and efficient method for gene delivery to a wide variety of cells, such as, Human bone marrow mesenchymal stem cells [65],

Human astrocytoma cells [66] and Human umbilical cord blood-derived mesenchymal stem cells (hUCB-MSCs) [67].

Even though these non-viral methods have shown to be effective and advantageous, it is important to optimize these technologies to allow better *in vivo* and *in vitro* transfection efficiency and permit the development of new therapeutic strategies. These improvements involve not only the development of new gene transfer technologies, but also the enhancement of transfection vectors that need to overcome many extra- and intracellular barriers.

1.6. Minicircles: The future of gene therapy?

Upon administration there are a number of extra- and intracellular systems that can impair gene delivery. Extracellularly, the vectors can be sequestrated in first pass organs (e.g. lung and liver) or affected by the extracellular matrix [68]. Intracellularly, the vectors encounter two distinct cytosolic barriers: a diffusional and a metabolic barrier. The diffusional barrier is related to the size-dependent deceleration of the vectors which might lead to the emergence of plasmid aggregates and an increase of the cytoplasm viscosity. The metabolic barrier is related to the presence of calcium-sensitive cytosolic nucleases that degrade foreign DNA [68-69]. The nuclear envelope represents the last barrier to be surpassed and to diffuse through the nuclear envelope the vectors must carry a nuclear localization sequence (NLS) to pass through the nuclear pore complex (NPC) or be transfected in dividing cells to gain access to the expression machinery after nuclear disassembly during mitosis [70].

To overcome these barriers many laboratories have been committed to the development of more effective plasmid vectors. Conventionally, pDNA is constituted by a mammalian expression cassette and a bacterial backbone consisting of an antibiotic resistance gene and an origin of replication for production in bacteria. To avoid degradation pDNA should be stable and mainly in the supercoiled form and free of contaminating factors (e.g. bacterial DNA, RNA and proteins). Many of the most recent advances in plasmid technology involve the substitution of the conventional polyadenylation (polyA) signals with more effective polyA sequences (e.g. Bovine growth hormone (BGH) polyA and SV40 polyA), that extend the half-life of supercoiled pDNA thus preventing the transformation into a circular form and exposure of secondary structures to the host nucleases [71], and the development of CpGfree plasmids. Unmethylated CpG motifs are predominantly present in bacterial DNA and therefore, are also common in bacterial derived pDNAs. These motifs are recognized by Toll-Like receptor 9 (TLR) positive cells (e.g. Dendritic cells) which activate host defense mechanisms triggering innate and acquired immune responses [72]. Transfection of CpGfree based pDNA has proven to yield high transgene expression *in vivo* and *in vitro* hence allowing sustained expression [73].

The real breakthrough in the vector upgrading was the development of the minicircle technology. Minicircle DNAs are small sized circular molecules, derived from plasmid DNA, that lack the bacterial backbone that triggers immune responses, alters gene expression and might potentiate the silencing of the encoded transgene. This technology consists on the construction of a parental plasmid that carries the expression cassette flanked by two recognition sites of a site-specific recombinase (e.g. λ derived recombinase; Cre rec.; FLP rec.) which is expressed and divides the parental plasmid into two molecules: a miniplasmid

that carries the bacterial backbone and a minicircle that carries the expression unit. One of the major drawbacks of minicircle technology was, until recently, the difficult and expensive purification procedure of these vectors [62]. To overcome these hardships, Chen and coworkers developed a new method that degrades the remaining miniplasmid and parental plasmids *in vivo* by the action of a restriction enzyme (*Sce*I), hence allowing a more effective purification [74], and more recently, the development of a robust minicircle production system permitted the establishment of a rapid and inexpensive protocol for production of minicircles [75]. When compared to regular plasmids, minicircles display a 10- to 10,000-fold improvement in long-term transgene expression *in vivo* [76-77], and, further improvements in their formulation, e.g. addition of scaffold/matrix attachment region (S/MAR), enhances transgene expression and persistence [78]. Altogether, this data confirm that minicircles offer a new concept in highly efficient and safe non-viral gene transfer, and in the future, they will represent the preferred system for gene delivery for clinical and therapeutic applications.

In this work, microporation conditions were optimized for gene delivery to NSCs for the use of two electroporation buffers, RB, the buffer provided by the manufacturer, and HMB, a buffer previously prepared at the laboratory. Furthermore, transfection efficiency was tested and compared using minicircles and pDNAs of different sizes and CpG content. Stem cell potential was investigated by evaluating the survival, proliferation, and differentiation potential of transfected cells and the number of copies of vector DNA was assessed in each case, more specifically, after Minicircle, pCMV-GFP and pVAX-eGFP transfection and the optimal dose of vector DNA for gene delivery to NSCs was determined. These results strongly suggest that there is a CpG dependent episomal transgene silencing in transfected NSCs and that minicircles are the vectors that give rise to the highest levels of gene expression without influencing the cell traits of NSCs.

2. Aim of Studies

This study was fully accomplished at Stem Cell Bioengineering Laboratory in Institute for Biotechnology and Bioengineering at Instituto Superior Técnico.

This work focused on the following points:

- Optimization of microporation conditions for gene delivery to NSCs by evaluating the effect of voltage, pulse duration, electroporation buffer and DNA amount.
- Evaluation of the GFP expression levels upon transfection of CGR8-NS cells with CpGfree plasmids.
- Comparison of the use of different gene vectors with different CpG content, more specifically, minicircles, pCMV-GFP and pVAx-eGFP in NSCs transfection – evaluation of cell viability, percentage of GFP expressing cells, proliferation kinetics and morphological traits.
- Quantification of the number of vector copies inside each nucleus after transfection with minicircle, pCMV-GFP and pVAX-eGFP, and determination of the ideal dose of vector after which transgene expression saturates.
- Evaluation of dilution kinetics of each vector – quantification of the number of vector copies inside the nucleus after transfection with minicircles, pCMV-GFP and pVAX-eGFP at specific points for 7-10 days.
- Differentiation of CGR8-NSCs – effect of transfection on differentiation potential.

The results obtained by this study will certainly be useful for future gene delivery applications in Neural Stem Cells, in particular, for the development of tissue regeneration applications and gene therapies for the treatment of neurodegenerative diseases or brain cancer where a transient expression of a gene of interest might be necessary.

3. Materials and Methods

3.1. Plasmids and Minicircles

3.1.1. Plasmids and Minicircles encoding GFP

The transfection vectors MC07.CMV-GFP (2257 bp), that will be referred as MC-GFP, and pCMV-GFP plasmid (3487 bp), both carrying the same GFP gene under the control of the cytomegalovirus (CMV) promoter and the SV40 polyadenylation sequence, were purchased from Plasmid factory (Bielfield, Germany). MC-GFP is a bacterial backbone vector consisting only on a mammalian expression cassette and pCMV-GFP is its correspondent plasmid which contains, apart from the expression cassette, an origin of replication and a Kanamycin resistant gene for prokaryotic selection. The pVAX-eGFP plasmid (3697 bp) was obtained by the modification of the commercial plasmid pVAX1lacZ (Invitrogen, 6050 bp) by replacement of the lacZ reporter gene with the enhanced Green Fluorescent protein gene (eGFP)(**Supplementary Fig.1**). The details of this construction are described elsewhere [1] and this plasmid was isolated and purified from a pVAX-eGFP transformed E. coli strain stored at -80 ºC.

3.1.2. Construction of CpGfree plasmids encoding GFP

a) CpGfree plasmid

The CpGfree plasmid (3049 bp, Invivogen) is a commercial vector consisting of elements devoid of CpG dinucleotides and Dam methylation sites (GATC). This plasmid contains: a R6Kγ origin of replication, a E2MK promoter, a Zeocin^{TM} resistance gene, and in the eukaryotic expression vector the promoter combines the mouse CMV enhancer, the human elongation factor 1 alpha core promoter and 5'UTR containing a synthetic intron, the late SV40 polyadenilation signal, matrix attachment regions (MARs) and a multiple cloning site (MCS).

b) Reconstitution of E. *coli* GT115 strain

The reconstitution of E. *coli* GT115 (provided with pCpGfree) was performed by adding 1 ml of LB medium to the tube containing the strain and incubation for 5 minutes at room temperature. The cell suspension was then mixed for 2 minutes and 100 µl of this suspension was plated in LB-Agar and incubated overnight at 37ºC. The resulting colonies were used to prepare competent cells (see below section 3.1.4).

c) Cloning of eGFP into CpGfree plasmids

The eGFP gene was amplified from the pVAX-eGFP vector. Briefly, 100 µl of E. *coli* transformed with pVAX-eGFP plasmids was inoculated in 5 ml falcons supplemented with 50 µg/ml Kanamycin and grown overnight at 37ºC and 250 rpm. The plasmid was then purified according to the protocol described in section 3.1.6 and its integrity verified through enzymatic digestion with *Hind*III and Agarose gel electrophoresis analysis. The eGFP gene was amplified by Polimerase Chain Reaction (PCR), using the following primers: *NcoI*-GFP-Fwd, 5'- AAACCATGGATGGTGAGCAAGGGCGA -3'; and GFP-*NheI*-Rev, 5'-TTTGCTAGCTTACTTGTACAGCTCGTCCATGCC -3' (STAB Vida). Each 50 µl of final reaction volume contained 10 ng of pVAX-eGFP, 10 µM of each primer, 25 µl of KOD Hot Start Master Mix (Novagen ®), and 20 µl of Distilled H_2O. The reaction was subjected to the following conditions: 5 min at 95ºC, 35 cycles of 30 s at 95ºC, 60 s at 60ºC and 90 s at 72ºC and 5 min at 72ºC. The amplification of the eGFP fragment was assessed through Agarose gel electrophoresis analysis and its purification was made using a DNA extraction and purification from Agarose gel kit (NZYTECH). The CpGfree-eGFP plasmid was then constructed through enzymatic restriction with *Nco*I and *Nhe*I and subsequent insertion of the eGFP reporter gene using T4 DNA Ligase. The construction was later confirmed through double enzymatic digestion with *Nco*I and *Nhe*I and Agarose gel electrophoresis analysis. The production and purification of this plasmid is described in section 3.1.8.

3.1.3. Production of Minicircles

a) Propagation of the Parental plasmid

The Minicircle DNA vector technology was purchased from System Biosciences (SBI; Mountain View, California) and the propagation of the Parental plasmid (PP-DNA, ≈7.8 Kb) was performed in an E. *coli* XLlgold strain and in an engineered E. *coli* ZYCY10P3S2T strain (provided by the manufacturer) as described below (Section 3.1.5).

b) Transformation of the Parental plasmid into E. *coli* ZYCY10P3S2T

The Transformation of the PP-DNA into E. *coli* ZYCY10P3S2T was performed as described by the manufacturer. Succinctly, 2 µg of MC-DNA was added to 100 µl of cells, incubated on ice for 30 minutes and at 42ºC for 30 seconds. The cell suspension was then placed on ice for 2 minutes after which 500 µl of S.O.C. medium supplemented with Kanamycin (50 µg/ml) was added. The mixture was then incubated for 60 minutes at 37ºC and 225 rpm. Afterwards, the cells were centrifuged for 10 minutes at 4000g, resuspended in 100 µl of S.O.C medium, plated on LB-Agar with 50 µg/ml of Kanamycin and incubated overnight at 37ºC. Some colonies were then harvested and cultured overnight, at 37ºC and

250 rpm, in 5 ml LB falcons with antibiotics. The presence of the PP-DNA was assessed through agarose gel electrophoresis analysis after simple enzymatic digestion with *Hind*III.

c) Induction assays for minicircle production

On day 1 in the morning, cells from a PP-DNA transformed colony was grown in 5 ml LB supplemented with 50 µg/ml of Kanamycin and incubated at 37ºC and 250 rpm. In the evening, 100 µl of cell suspension was inoculated in 400 ml or 25 ml of TB medium supplemented with Kanamycin. On day 2 in the morning, the OD was registered and a minicircle (MC) induction mix was prepared and 4 induction assays were performed. The first 2 assays were performed as described by the manufacturer protocol and involved the combination of the MC induction mix, composed of 400 ml or 25 ml of LB supplemented with 4% 1N NaOH and 0.1% of a 20 % L-Arabinose (Sigma) solution, with the overnight culture. In the third induction assay the 25 ml of the overnight culture was split in 2 flasks and one of the cultures was combined with 25 ml of MC induction mix while the second was combined with 12,5 ml of TB medium and 25 ml of MC induction mix. The fourth assay involved the division of the 25 ml of the overnight culture in 2 flasks and the addition of 25 ml of MC induction mix to each flask: one of the cultures was mixed with MC induction mix supplemented with 1% of 20% L-ara and the other was combined with MC induction mix supplemented with 2% of 20% L-ara. All the cultures were incubated at 30ºC with shaking at 250 rpm for 7 hours or longer. The OD was registered every 2,5 hours and the presence and integrity of the MC-DNA and MC was assessed through agarose gel analysis.

3.1.4. Preparation of E. *coli* competent cells

A single colony of the desired E. *coli* strain (GT115 and ZYCY10P3S2T) was isolated and grown overnight, at 37ºC and 250 rpm, in a falcon containing 5 ml of LB.In the morning the Optical Density measured at 600 nm (OD) was measured and the appropriate volume of cell suspension was added to 20 ml of LB medium to start growth at OD = 0.1. , followed by incubation at 37ºC and 250 rpm. Simultaneously a TSS solution was prepared as follows: 10 ml of 40 g/L LB, 1 ml of DMSO, 1 ml of 1M $MgCl_2$, 2 g PEG8000 and H_2O until 20 ml; the pH was adjusted to 6.5 and the solution was sterilized by filtration . When the OD of the cell suspension reached the value of 0.9, the content of the flask was divided into falcons and centrifuged at 1000 g for 10 minutes. The pellet was resuspended in 5 ml of cold TSS (0.1 V) and incubated on ice for 10 minutes. The suspension was divided into eppendorfs (100 µL/eppendorf), and stored at -80ºC.

3.1.5. Transformation of plasmids into E. *coli*

The transformation of E. *coli* competent cells with the desired plasmids (E. *coli* GT115 with pCpGfree and pCpGfree-eGFP and E. *coli* XLlgold with PP-DNA) was performed using a Heat Shock protocol. Briefly, 2 µg of plasmid was added to 100 µl of cells, incubated for 15 minutes on ice and at 42ºC for 1 minute. 900 µl of sterile LB medium supplemented with antibiotics (25 µg/ml of Zeocin for pCpGfree and pCpGfree-eGFP and 50 µg/ml of Kanamycin for MC-DNA) was then added to the mixture and a 40 minutes incubation, at 37ºC and 250 rpm, was performed. Afterwards, the cells were centrifuged at 4000 rpm for 10 minutes. The pellet was resuspendend in 100 µl of LB and plated overnight, at 37ºC, in LB Agar plates with respective antibiotics. Some colonies were then harvested and cultured overnight, at 37ºC and 250 rpm, in 5 ml LB falcons with antibiotics. The presence of the plasmids and their integrity was evaluated through agarose gel electrophoresis after a simple and a double enzymatic digestion of the pCpGfree and pCpGfree-eGFP with *Nhe*I, and *Nco*I and *Nhe*I respectively, and a simple enzymatic digestion of MC-PP with *Hind*III.

3.1.6. Purification of plasmids

The purification of plasmids (pCpGfree; pCpGfree-eGFP; pVAX-eGFP; PP-DNA and respective Minicircle (MC)) was performed using a miniprep kit (Promega), according to supplier's protocol.

3.1.7. Preparation of plasmid banks

Colonies of transformed E. *coli* strains with the desired plasmids (E. *coli* GT115 transformed with pCpGfree and pCpGfree-GFP; E. *coli* XLlgold and ZYCY10P3S2T transformed with PP-DNA) were harvested and inoculated in falcons containing 5 ml of LB supplemented antibiotics and grown overnight, at 37ºC and 250 rpm. Afterwards, 150 µl of cell suspension was inoculated into new 5 ml LB falcons with antibiotics in order to start the new growth with a OD=0.1. When the OD reached the value of 0.8 (after 4 hours of incubation at 37ºC and 250 rpm), the suspension was divided into criovials containing 200 µL of glycerol by adding to each vial 800 µL of the cell suspension. The vials were stored at -80ºC.

3.1.8. Endotoxine free purification of plasmids

Aliquots containing E. *coli* strains transformed with the plasmids pVAX-eGFP and pCpGfree-eGFP were added to 2 L flasks with 250 ml of LB medium supplemented with antibiotics and allowed to grow overnight at 37ºC at 250 rpm. Plasmid DNA was then purified using an Endotoxin-free Plasmid DNA Purification kit (Machery-Nagel) according to manufacturer protocol and plasmid concentration was determined using a NanoDrop equipment (Digital Bio) by spectrophotometric measurements at 260 nm.

3.2. Cell lines

3.2.1. Culture and expansion of HEK293T cells

Criovials preserved at -80ºC, containing Human Embryonic Kidney (HEK) 293T cells (ATCC-LGC Nr: CRL-11268; Middlesex, UK) were thawed by resuspending their content in 6 ml of Dulbecco's Modified Eagle Medium (DMEM, 1g/L Glucose, Gibco) supplemented with 10% fetal bovine serum (FBS, Gibco) and 1% (v/v) penicillin/streptomycin (Gibco). The mixture was then centrifuged at 1250 rpm for 5 minutes, and the pellet was ressuspendend in 6 ml of DMEM (10% FBS, 1% PenStrep). The number of cells and their viability was determined by Trypan blue staining (Gibco). Afterwards 7.5 x 10^5 cells were cultured in 75 cm^2 T-flasks (FALCON®) (10000 cells/cm^2) and grown in adherence, under static conditions, at 37ºC and 5% CO_2-humidified atmosphere. Sub-confluent cells were collected and used for transfection with pCpGfree-eGFP and pVAX-eGFP. In brief, HEK293T cells were washed with 10 ml of Phosphate buffered saline (PBS) solution (Gibco) and harvested with 4 ml of Trypsin 0.25% (Gibco) after incubation for 3 minutes at 37ºC and 5% CO_2-humidified atmosphere. The cells were then resuspendend in 6 ml of complete medium and centrifuged at 1250 rpm for 5 minutes and the pellet was resuspendend in culture medium. The number of cells and their viability was determined by Trypan blue staining and the cells were transfected by microporation.

3.2.2. Culture and expansion of Neural Stem Cells

CGR8-NS cells, derived from ES cell line CGR8 (Welcome Trust Centre for Stem Cell Research in Cambridge, United Kingdom) were thawed by swiftly submerging the criovials in a water bath at 37ºC and by resuspending the cells with RHB-A (Stem Cell Sciences) medium supplemented with 15 ng/ml of EGF and FGF-2 (Peprotech) and 1% of penicillin/streptomycin (100 µg/ml) (Gibco) or with DMEM/F-12 (Gibco) supplemented with 0,8 g/ml of Glucose, 1% N-2 supplement (Gibco), 20 µg/ml insulin (Sigma), 1% of penicillin/streptomycin and 15 ng/ml of EGF, FGF-2 and B27 (Invitrogen). The mixture was centrifuged at 1000 rpm for 3 minutes and the pellet was resuspendend in 5 ml of culture medium. Cell viability was then assessed through Trypan blue assay. The cells were seeded in 25 cm^2 T-flasks (10000 cells/cm^2) and grown under static conditions at 37ºC and 5% CO_2-humidified atmosphere. When the cells reached sub-confluence they were harvested with 1 ml of Accutase (Sigma) and incubated at 37ºC and 5% CO_2-humidified atmosphere for 3 minutes. Afterwards they were resuspendend in growth factor supplemented medium and centrifuged at 1000 rpm for 3 minutes. The pellet was then resuspended in culture medium and the cell number and viability was assessed by Trypan blue staining. The cells were then used directly in transfection assays or cultured in T_{75} flasks and grown under static conditions

at 37ºC and 5% CO^2-humidified atmosphere. When the T_{75} flasks exhibited a 70-80% cell confluence, NS cells were harvested and used for transfection.

3.3. Gene transfection by microporation

Cells were resuspendend in Resuspension buffer (RB; provided by the equipment manufacturer (Digital Bio)) or in Home Made Buffer (HMB; prepared at IBB/IST whose formulation is described elsewhere [79]) and incubated with a specific amount of vector DNA (pVAX-eGFP; pCPGfree-eGFP; MC-GFP, pCMV-GFP) on ice. Microporation was accomplished using a Microporator MP100 (DigitalBio/(Neon) Invitrogen). DNA amount is referred when appropriate and used within 200 000 CGR8-NS cells/ 10 µl of RB or HMB and 150 000 HEK293T cells/10 µl of HMB. After microporation, the 10 µl of cell suspension was seeded as follows: HET293T cells were plated into a well of a 12- well culture plate with pre-warmed medium without antibiotics; CGR8-NSCs for RT-PCR assays were seeded into a 24-well culture plate with pre-warmed medium without antibiotics and CGR8-NSCs for cell proliferation kinetics analysis were added to 100 µl of pre-warmed medium without antibiotics and equally divided into 2 wells of a 24-well culture plate containing culture medium under the same conditions. Afterwards the cells were incubated at 37ºC and 5%CO_2-humidified atmosphere for 24h after which the medium was replaced by complete medium. For the long term gene expression assays the cells maintained under the previously mentioned conditions for 10 days, and harvested on days 1, 3, 4, 7 and 10. On day 4 of cell proliferation kinetics assays (section 4.5.2) or on days 4 and 7 in RT-PCR assays (section 4.6.3) cells for the subsequent days were harvested and replated into two wells of a 24- or 12- well plate, respectively. The optimization assays were made with resuspension of CGR8-NS cells in RB and HMB and incubation with pVAX-eGFP and pVAX-eGFP or MC-GFP respectively. The cells were microporated using a different combination of programs and harvested and analyzed after incubation for 24h at 37ºC and 5%CO_2-humidified atmosphere. In all the experiments, non-microporated (NM) cells were used as controls and each assay was repeated at least twice.

3.4. Analysis after transfection

3.4.1. Fluorescence microscopy imaging

Transfected and immunostained cells were visualized using a fluorescence optical microscope Leica DMI 3000B (Leica Microsystems GMbH) and digital images were obtained with a digital camera Nikon DXM 1200F. Fluorescence images were acquired with either green or red filters, depending on the purpose, and a minimum of 2 microscopic fields at 100x, 200x and 400x magnification were scored.

3.4.2. Flow cytometry

The percentage of GFP expressing cells and level of expression were measured by flow cytometry in the FACSCalibur equipment (FACSCalibur Becton Dickinson). The cells in each well were harvested by transferring the medium to FACS tubes and adding Accutase to each well. After incubation at 37ºC and 5%CO_2-humidified atmosphere, the cells were resuspendend in medium supplemented with growth factors and added to the FACS tubes. A centrifugation (1000 rpm, 3 minutes) was performed and the pellet was resuspendend in 100 µl of culture medium. After counting, cells were fixed in 500 µl of 4% Paraformadehyde (PFA) and analyzed by flow cytometry. A minimum of 1000 events were gated and statistically evaluated by CellQuest software (BD Biosciences).

3.4.3. Cell viability, recovery, yield and transfection efficiency

The number of living and dead cells was assessed by Trypan blue exclusion method and cell viability, recovery and yield of transfection values were determined using the following equations:

$$\text{Cell Viability (\%)} = \frac{\text{Total number of Viable}}{\text{Total number of cells}} \times 100$$

$$\text{Cell Recovery (\%)} = \frac{\text{CAt}}{\text{CAc}} \times 100$$

$$\text{Yield (\%)} = \frac{\%\text{GFP}^{+} \text{ cells x CAt}}{\text{CTc}} \times 100$$

CAt corresponds to the number of viable transfected cells, CAc is the number of viable non-transfected cells (control) and CTc is the number of total cells (control).

3.4.4.Cell proliferation kinetics

CGR8-NSC were stained using PKH26 Red Fluorescent Cell Linker kit (Sigma) prior to transfection as described before [80]. Cells were then microporated with 2.0 x 10^{11} molecules of vector DNA (pVAX-eGFP; pCMV-GFP; Minicircle-GFP) as previously described (Section 3.3.). Cells were analyzed by flow cytometry (FACSCalibur Becton Dickinson) and cell viability was calculated on days 1, 3, 4, 7 and 10 after transfection. The number of divisions or generations within a specific subset was assessed by analyzing the decrease of fluorescence overtime on a proliferation wizard module of the ModFit Software (Becton Dickinson) in the flow cytometer equipment. Non-Microporated cells were used as controls.

3.4.5.Real Time PCR for quantification of vector DNA copies

Quantitative Real-Time PCR (RT-PCR) was performed on microporated CGR8-NS cells incubated with a variable amount (0,1; 0,5; 0,8; 1; and 1,5 µg) of vector DNA (pVAX-eGFP; pCMV-GFP; MC-GFP) after 24h of incubation and on CGR8-NS cells incubated with 2.0 x 10^{11} molecules of vector DNA (PVAX-eGFP; pCMV-GFP; Minicircle-GFP) on days 1, 4, 7 and 10. PCR reactions were carried out in a Roche LightCycler™ detection system using the FastStart DNA Master SYBR Green I kit (Roche, Basel) by amplification of a 108 bp sequence within the eGFP gene (forward primer: 5'- TCGAGCTGGACGGCGACGTAAA-3' and reverse primer: 5' – TGCCGGTGGTGCAGATGAAC – 3'; STABVida) and a 80 bp sequence within the GFP gene (forward primer: 5'-TGAACGGCGTGGAGTTCGAG-3' and reverse primer: 5'-GCTCTTCATCTTGTTGGTCATGCG-3'; STABVida). Each 20 µl of final reaction volume contained 2 µl of the 10x SYBR Green mixture, 0,4 µM of each primer, 3 mM of MgCl2, 2-5 µl of sample (corresponding volume to 20 000 NSC) and 9,4 µl of PCR grade water. The amplification of the sequences within the eGFP and GFP genes was carried out at 95ºC for 10 min, followed by 40 cycles of 10 s at 95ºC, 5 s at 55ºC and 7 s at 72ºC and at 95ºC for 10 min, followed by 40 cycles of 10 s at 94ºC, 5 s at 53 ºC and 7 s at 72ºC respectively.

Calibration curves were constructed by adding serial dilutions of vector DNA standards (pVAX-eGFP; pCMV-GFP; MC-GFP) to a suspension of NM CGR8-NS cells (20 000 cells per reaction). These samples were then mixed with the other PCR reagents as described above. One negative control was included in the analysis containing the same amount of NM cells and PCR grade water.

3.5. Differentiation of Neural Stem Cells

Neuronal differentiation was accomplished as previously described by Spiliotopoulos *et al* [31]. Briefly, cells were transfected (1.5 x 10^5 – 2.0 x 10^5 cells/cm^2) with 2.0 x 10^{11} molecules of pVAX-eGFP and plated on a 6-well plate and incubated for 3 days at 37ºC and 5%CO_2-humidified atmosphere. Non-microporated cells and microporated cells without DNA were used as controls. Almost confluent cultures were then dissociated with Accutase, counted and plated on a 6-well plate using RHB-A medium supplemented with 1% B27, 0,5 % N-2 Supplement and 10 ng/ml FGF-2, at a density of 1.0 x 10^5 – 1.5 x 10^5 cells/cm^2. After 3 days at the previously mentioned conditions, cells were harvested with accutase, counted and plated at a density of 5 x 10^4 – 7.5 x 10^4 cells/cm^2 on a Laminin (Sigma) – coated (3 mg/ml for 4h at 37ºC) 24-well plate in medium composed of a 1:1 mixture of RHB-A and Neurobasal media (Invitrogen) supplemented with 0.5 % N-2 supplement, 1% B27, 10 ng/ml FGF-2 and 20 ng/ml BDNF (Invitrogen). After 3 days, the medium was replaced with medium composed of a 1:3 mixture of DMEM/F12 and neurobasal media containing 0.5% of N-2 supplement, 1% B27, 6,7 ng/ml FGF-2 and 30 ng/ml BDNF. Three days later the medium was replaced with fresh media with a reduced amount of FGF-2 (5 ng/ml) and cells were maintained in these conditions for an additional 12 days with partial change of medium every 3 days. Neuronal differentiation was then assessed by fluorescence microscopy imaging after staining with Alexa Fluor 488® labeled Neuronal Class III b-Tubulin (TUJ1) (Covance, dilution 1:2000) and DAPI (Sigma-Aldrich, dilituion 1:10000).

4. Results

4.1. Production of CpG-free plasmids

The commercial plasmid CpGfree (3049 bp) is a bacterial derived expression cassette which was modified in order to be completely devoid of CpG dinucleotides and DAM sites to prevent prokaryotic methylation. This plasmid contains an expression cassette, which comprises a modified promoter (CMV enhancer is combined with the EFI-a core promoter and 5'UTR containing a synthetic intron) and the late SV40 polyA signal, and sequences for expression in E. *coli*, such as, the R6Kγ *ori*, the EM2K promoter and the Zeocin selectable marker. Due to the presence of the modified R6Kγ *ori,* which can only be activated by the protein π which is encoded by the *pir* gene, this plasmid was propagated and purified from a *pir* mutant E. *coli* GT115 strain that encodes a mutant protein π that recognizes the modified origin of replication, and allows plasmid replication (**Fig.1A**).

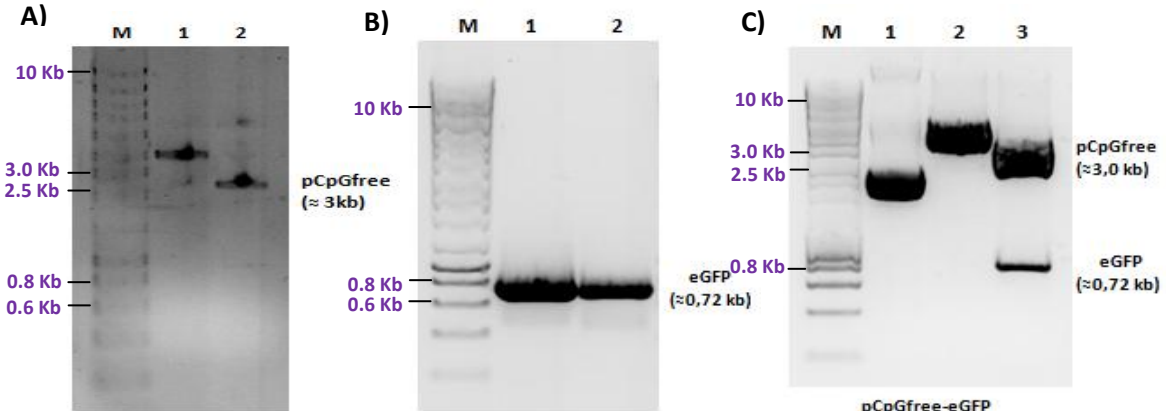

Figure 1: Agarose gel electrophoresis of pCpGfree and pCpGfree-eGFP construction.

A) Confirmation of E. *coli* GT115 transformation with pCpGfree. Lane 1 represents supercoiled pCpGfree and 2 the pCpGfree after restriction with *Nhe*I. **B)** Confirmation of eGFP amplification through PCR. Lanes 1 and 2 represent the amplified eGFP fragment. **C)** Confirmation of the construction after simple and double enzimatic restriction. Lane 1 represents supercoiled pCpGfree-eGFP, 2 represents pCpG-eGFP after restriction with *Nhe*I (one band ≈3,7kb) and 3 represents pCpGfree and eGFP after double enzymatic restriction. M corresponds to NZYDNA III Ladder (NZYTech).

To construct the CpGfree-eGFP plasmid, the eGFP sequence was amplified from pVAX-eGFP through PCR. For this purpose the primers *NcoI*-GFP-Fwd and GFP-*NheI*-Rev were designed for the amplification and introduction of the *Nco*I and *Nhe*I restriction sites into the eGFP sequence. The resulting fragments were identified through gel agarose electrophoresis (**Fig.1B**), isolated and engineered into the MCS of pCpGfree by the action of T4 ligase. The construct was amplified in E. *coli* GT115 and the ligation was confirmed through agarose gel analysis after simple and double enzymatic digestion with *Nhe*I, and *Nhe*I and *Nco*I respectively, that originated one band of linearized pCpGfree-eGFP (≈3,7 kb) (**Fig.1C, lane 2**) and two distinct bands that corresponded to the CpGfree plasmid (≈3 kb) and the eGFP sequence (≈0,72 kb) (**Fig.1C, lane 3**).

4.2. Long-term analysis of pCpGfree-eGFP transfected cells

The CpGfree commercial plasmids were developed to allow high and sustained expression of transgenes *in vitro* and *in vivo*. These plasmids are completely devoid of CpG motifs that are recognized by TLR9 which trigger immune responses prompting transgene silencing. To assess the transfection efficiency of pCpGfree-eGFP and its maintenance overtime, HEK293T cells and CGR8-NC cells were microporated with 1 µg and 0.8 µg of pCpGfree-eGFP and pVAX-eGFP respectively, corresponding to the same number of molecules and equal to 2.4 x 10^{11} and 2.0 x 10^{11} respectively. Cells were analyzed at different points in time after transfection by flow cytometry and GFP expression was compared for cells transfected with pVAX-eGFP and pCpGfree-eGFP.

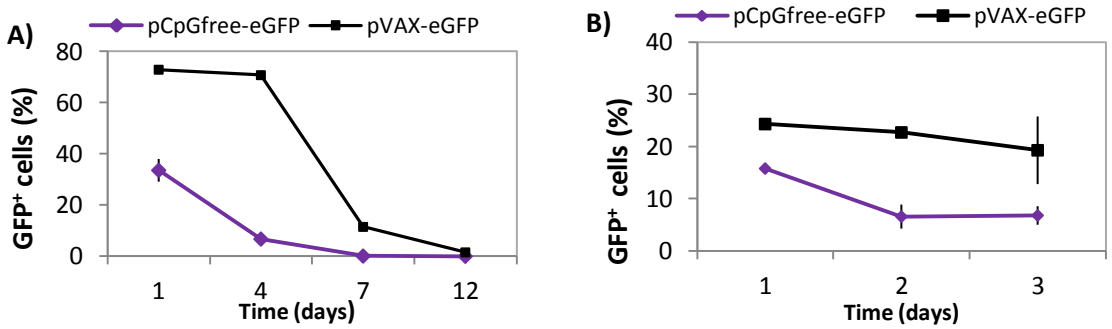

Figure 2: Transfection efficiencies of HEK293T cells and CGR8-NS cells using pCpGfree-eGFP and pVAX-eGFP.

A) HEK193T cells were transfected with 1 µg of pDNA, using 1250V/20ms/1p. Cells were harvested on days 1, 4, 7 and 12 and GFP expression was assessed through flow cytometry. The results are expressed as the mean ± SEM of 2 replicas of the same experiment. **B)** CGR8-NS cells were transfected with 0.8 µg of pDNA, using 1500V/20ms/1p. Cells were harvested on days 1, 2 and 3 and GFP expression was assessed through flow cytometry. The results are expressed as the mean ± SEM of 2 replicas of the same experiment. Non-microporated cells served as controls (not shown).

Long term analysis of transfected HEK293T and CGR8-NS cells showed a lower percentage of pCpGfree-eGFP transfected cells and a faster decay of GFP expression compared with pVAX-eGFP transfected cells (Fig.3). In pVAX-eGFP transfected HEK293T cells the GFP expression was maintained at high expression levels (over 70%) in the first 4 days, and decreased until it reached its minimum level at day 12. In pCpGfree-eGFP transfected HEK293T cells the highest expression level was observed on day 1 (≈ 34%) and showed a fast decrease until it ceased on day 7 (**Fig.2A**). In CGR8-NS cells the expression was assessed for 3 days and is characterized by lower levels of GFP^+ cells and faster GFP expression decay when compared with pVAX-eGFP transfected cells (**Fig.2B**). These results indicate that pCpGfree-eGFP transient expression *in vitro* is fast diluted, suggesting that the problem might be within the pCpGfree formulation, more specifically, the modified promoter that might be weaker compared to the promoter present in pVAX-eGFP. Due to these results, the use of pCpGfree-eGFP was discarded in further experiments.

4.3. Induction assays for Minicircle production

The minicircle production protocol developed by Systems Biosciences was prepared after the procedure of Kay *et al*. [75] and relies on the production of minicircles in an engineered E. *coli* strain that harbors an arabinose-inducible system that leads to the expression of ϕC31 integrase and the SceI endonuclease. Upon arabinose induction the full-sized MC-DNA is separated into bacterial backbone (PP-DNA) and minicircle by the action of ϕC31 integrase, and the PP-DNA is degraded by the action of SceI endonuclease (**Supplementary Fig.2**).

To test minicircle induction conditions, four (I1, I2, I3 and I4) distinct induction assays were performed. In all the experiments, a PP-DNA engineered E. *coli* ZYCY10P3S2T colony was grown in LB on day 1 and incubated overnight in TB medium and the OD600 was registered in the morning before starting induction. According to the manufacturers protocol, on day 2 in the morning, the OD600 should be around 4 or 5, however, in all the performed experiments, the OD600 of the overnight culture was above 8 (OD600: I1= 9.4, I2 = 9, I3 = 8.6, I4 = 8.5) (**Table 1**). The first two induction assays (I1 and I2) were performed as described by the protocol, the OD600 was registered at specific points in time and the induction efficiency was evaluated through gel agarose electrophoresis after purification of DNAs as described in section 3.1.6. The results of both assays indicate that the culture reaches the growth stationary phase after 5 hours of induction, as described by the protocol, at an OD600 of around 7 (**Table 1**). However, the induction was not efficient, and in both cases, it was not possible to produce purified minicircle (at I1 it was not possible to identify any band that corresponded to minicircle, and at I2 production of minicircle was detected, however, the presence of full-sized PP-DNA was also identified) (**Fig. 3, I1 and I2**).

Table 1: OD600 values for the induction assays for the production of minicircles.

I1, I2, I3 and I4 represent the 4 assays performed and 0* corresponds to the OD600 value for the overnight culture on day 2 before induction, and the subsequent values were registered at specific hours throughout the induction.

I1		**I2**		**I3**			**I4**		
Time (h)	**OD600**	**Time (h)**	**OD600**	**Time (h)**	**OD600**		**Time (h)**	**OD600**	
					C1	**C2**		**C1**	**C2**
0*	**9.4**	**0***	**9**	**0***	**8.6**		**0***	**8.5**	
0	6.2	**3**	6.2	**0**	5.6	2.6	**0**	3.2	3.5
2.5	6.7	**4.5**	7.1	**2.5**	6.4	3.7	**5**	5.5	5.5
5	7.3	**6**	7	**5**	7.2	4.7	**7**	5.8	6
7	7.3	**9.5**	6.5	**7**	6.5	4.7	**24**	6.5	6.7

To test if the inefficient production of minicircles was due to starvation or insufficient arabinose quantity, two other induction experiments were performed with modifications in the provided procedure. In the third induction experiment (I3), to test the hypothesis of culture starvation, the overnight culture was split in two flasks and while one of the flasks was combined with MC induction mix (C1), the second was combined with fresh TB medium and MC induction mix (C2), and in the fourth experiment (I4), to test the effect of arabinose concentration, the overnight culture was split into two flasks and each was blended with MC induction mix with a 10- or 20- fold increase (C1 and C2 respectively) in the arabinose concentration suggested by the manufacturers protocol.

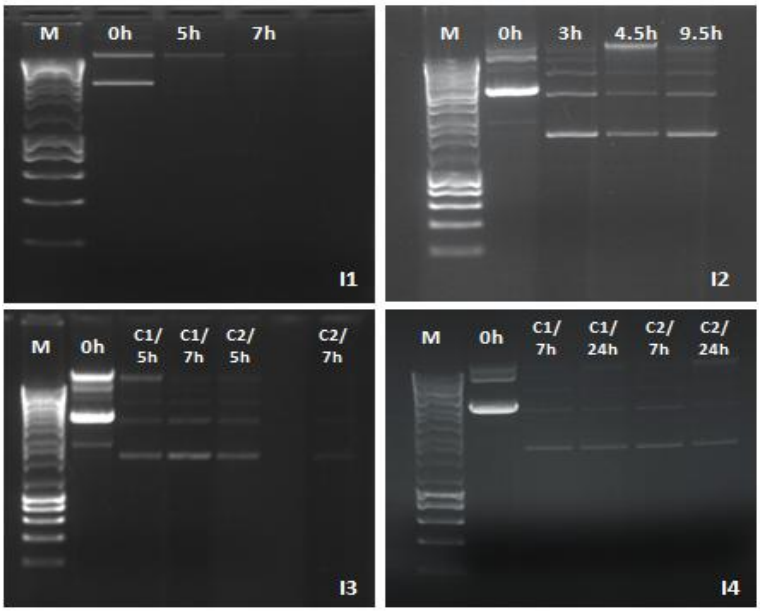

Figure 3: Agarose gel electrophoresis of the Minicircle induction assays.

I1) analysis of MC induction at 5 and 7 hours; **I2)** analysis of MC induction at hours 3, 4.5 and 9.5; **I3)** analysis of MC induction of cultures 1 and 2 at hours 5 and 7; **I4)** analysis of MC induction of cultures 1 and 2 at hours 5 and 24; In all the assays M corresponds to NZYDNA III Ladder (NZYTech) and 0h represents the isolated full-sized PP-DNA before the start of minicircle induction.

The results indicate that the stationary growth phase was achieved 5 (I3, C1 and C2) and 7 hours (I4, C1 and C2) after the start of induction at an OD600 of around 5 and 7 (**Table 1**). The agarose gel analysis shows that, even after providing more nutrients to the culture (I3) and increasing the arabinose concentration in the induction mix (I4) it was not possible to efficiently produce and purify uncontaminated minicircles (**Fig.3, I3 and I4**) because even after 24h of culture a band of parental plasmid was observed. Moreover, it seems that a low amount of corresponding minicircle was obtained. The obtained results suggest that the inefficient production of uncontaminated minicircles is a result of uncontrolled overgrowth, as it was evidenced by the high OD600 obtained in all the induction assays, and subsequent progressive cellular death of the PP-DNA engineered E. *coli* cultures caused by the lack of nutrients and space to sustain the high concentration of bacteria in the cultures.

4.4. Optimization of microporation conditions in NSC

4.4.1. Optimization of microporation conditions using RB

To determine the appropriate microporation conditions to achieve higher transfection efficiencies in CGR8-NSCs resuspended in RB, three different optimization assays were performed. In the first optimization assay 200,000 cells were resuspended in RB, microporated with 1 µg of pVAX-eGFP and transfected using different voltages: 1300, 1400, 1500, 1600 and 1700 V, with 20 ms of pulse duration and 1 pulse. Cells were analyzed after 24h for cell viability (**Fig. 4A**) and recovery (**Fig. 4B**). Yield of Transfection and GFP^+ cells were determined by flow cytometry (**Fig. 4C and D**).

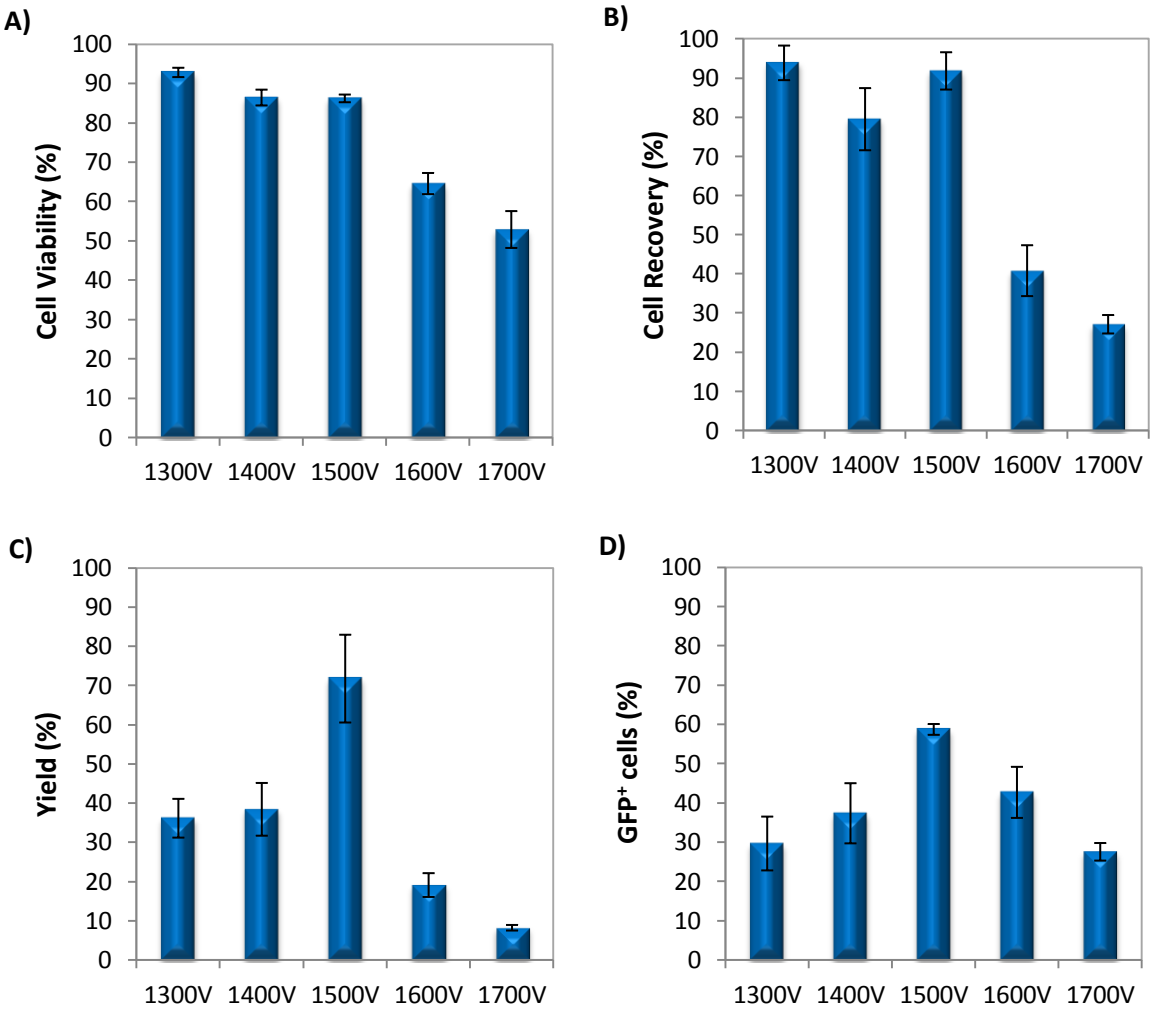

Figure 4: Transfection of CGR8-NSC resuspended in RB and microporated using 5 different voltages with 20 ms of duration and 1 pulse.

CGR8-NSCs were transfected with 1 µg of pVAX-eGFP and analyzed 24h after microporation by trypan blue exclusion method for **A)** cell viability, **B)** Cell recovery and flow cytometry for **C)** yield of transfection, and **D)** Percentage of cells expressing GFP; NM cells were used as controls (Control viability ≈92%, not shown) and the results are expressed as mean ± SEM of two independent experiments.

High cell viabilities and recoveries were obtained when using 1300 V (cell viability ≈93%; cell recovery ≈94%) and 1500 V (cell viability ≈86%; cell recovery ≈92%), however, the highest yield of transfection and percentage of positive GFP cells were obtained with 1500 V (Yield ≈72%; GFP^+ ≈60%). Overall, the results indicate that 1500 V might be an appropriate voltage to transfect CGR8-NS cells when using RB as electroporation buffer, therefore this voltage was determined for the posterior transfection assays.

In the second optimization assay 200,000 cells were resuspended in RB, microporated with 1 µg of pVAX-eGFP and transfected using different pulse durations (20 ms and 30 ms) with 1500 V as predetermined voltage and 1 pulse. Cells were analyzed after 24h for cell viability and recovery, percentage of GFP^+ cells (**Supplementary Fig. 3A**) and yield of Transfection (**Supplementary Fig. 3B**). Cell viability and recovery was higher for cells transfected using 20 ms of pulse duration (Cell viability and recovery ≈ 85-90%) compared to cells transfected using 30 ms (Cell viability ≈ 47%; Cell recovery ≈ 27%). The obtained results for the level of GFP^+ cells and yield of Transfection were consistent with the acquired cell viabilities and recoveries showing higher levels (GFP^+ cells ≈60%; Yield ≈52%) when using 20 ms as pulse duration. Given the obtained results, it is evident that using shorter duration pulses is more beneficial to obtain higher transfection efficiencies. Additionally, a new combination of settings, based on the decreasing of pulse duration from 20 to 10 ms and the increase of the number of pulses from 1 to 2, was tested, however, although results were slightly better than the ones obtained with 30 ms, they were not as good as the ones obtained with 1500V, 20 ms and 1 pulse (data not shown). With the previously described optimization assays it was possible to determine that, when using the electroporation buffer RB, the preferred condition to transfect CGR8-NS cells by microporation is 1500 V with 20 ms of pulse duration and 1 pulse.

The third optimization assay was performed to determine the ideal amount of plasmid vector to transfect CGR8-NS cells. For this purpose, 200,000 cells were resuspended in RB and microporated using increasing amounts of pVAX-eGFP (0.5, 0.8, 1.0 and 1.5 µg) at 1500V/20ms/1p as microporation condition. Cells were analyzed after 24h for cell viability (data not shown) and recovery (**Fig. 5B**), percentage of GFP^+ cells (**Fig. 5A**) and yield of Transfection (data not shown).

The increase in DNA amount caused a significant decrease in cell viability (from 92 to 59%, data not shown) however, the highest cell recovery level was obtained when using 0.8 µg of pVAX-eGFP (≈ 86%). These results were also evident when analyzing the yield of transfection that showed higher values for cells transfected with 0.8 µg of pDNA (≈ 40%). On

the other hand, the increase of DNA amount didn't seem to greatly affect the level of GFP transfected cells that showed similar values (≈50%) in all the tested amounts. Therefore, the pDNA quantity that showed the better results, 0.8 µg, was chosen for the subsequent experiments and studies.

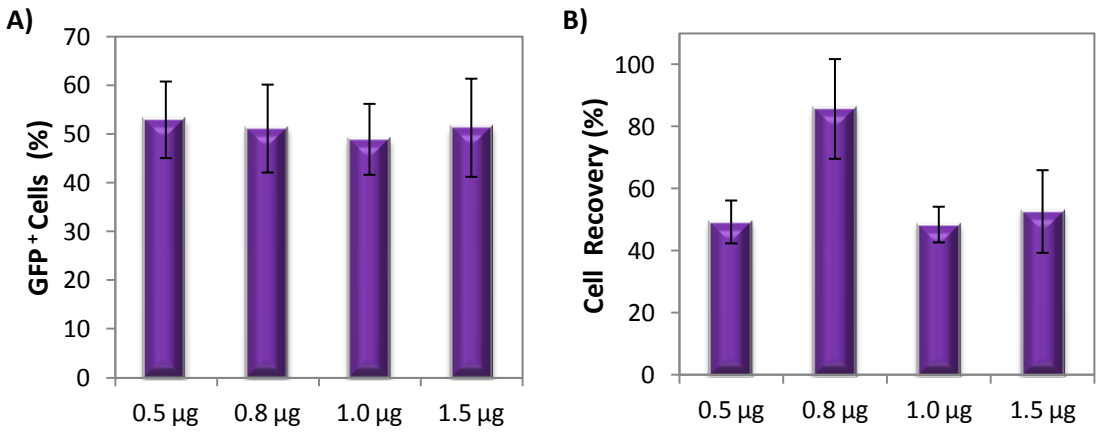

Figure 5: Transfection of CGR8-NSCs ressuspended in RB and transfected using different amounts of pDNA and 1500V/20ms/1p as microporation parameters.

CGR8-NSCs were transfected with 0.5, 0.8, 1.0 and 1.5 µg of pVAX-eGFP and analyzed 24h after microporation; **A)** % GFP^+ cells was assessed by flow cytometry and **B)** Cell recovery was assessed by trypan blue exclusion method. NM cells were used as controls (Control viability ≈92%) and the results are expressed as mean ± SEM of two independent experiments.

4.4.2.Optimization of microporation conditions using HMB

Another optimization assay was performed to determine the appropriate microporation conditions when resuspending CGR8-NS cells in another electroporation buffer. For this effect CGR8-NS cells were resuspended in HMB, a buffer that was previously prepared at the laboratory and proven to be efficient in microporation of HEK293T cells [79], and transfected with 2.0 x 10^{11} molecules of MC-GFP and pVAX-eGFP, which corresponded to 0.5 and 0.8 µg of vector DNA respectively, to avoid differences related to the number of vectors supplied. Cells were then microporated using different voltages (1600, 1700, 1800 and 1900V) with 20 ms and 1 pulse as microporation conditions. After 24h, the cells were analyzed and results were obtained for cell viability and recovery (data not shown), levels of GFP^+ cells and yield of Transfection (**Fig. 6**).

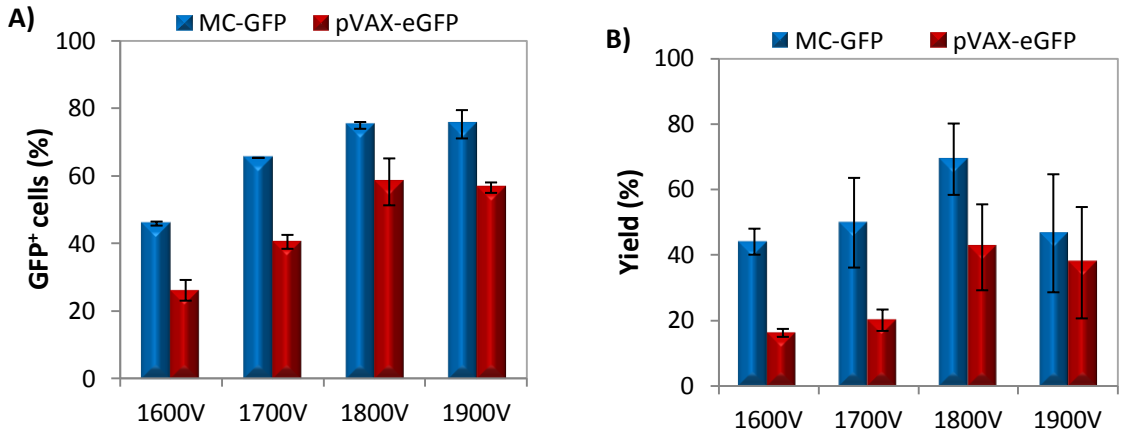

Figure 6: Transfection of CGR8-NSCs resuspended in HMB and microporated using different voltages with 20 ms of duration and 1 pulse.

CGR8-NSCs were transfected with 2 x 10^{11} of MC-GFP and pVAX-eGFP, and analyzed 24h after microporation by trypan blue exclusion method and flow cytometry; **A)** Percentage of GFP^+ cells and **B)** Yield of Transfection. NM cells were used as controls (Control viability ≈ 82%, not shown) and the results are expressed as mean ± SEM of three independent assays.

The obtained results show that cell viability and recovery slightly decrease with higher voltages for MC-GFP transfected cells (cell viability from ≈92 to 82%; cell recovery from ≈97 to 83%) and plummet for cells transfected with pVAX-eGFP (cell viability from ≈84 to 63%; cell recovery from ≈65 to 49%). As for levels of GFP^+ cells and yield of Transfection, the values rose significantly with the increase of the voltage until 1800 V, with GFP^+ levels ranging from 45 to 75% in MC-GFP transfected cells and 29 to 58% in pVAX-eGFP transfected cells and yields from 44 to 69% in MC-GFP transfected cells and 16 to 47% in pVAX-eGFP transfected cells. However, when using 1900V as microporation setting the levels of GFP transfected cells stabilized (**Fig. 6A**) and the yield of Transfection decreased (**Fig. 6B**) most probably as a result of the lower cell viabilities and recoveries obtained with this voltage. These results suggest that for resuspension of CGR8-NS cells in HMB, the preferred microporation condition is 1800V, 20 ms and 1 pulse.

4.4.3.Comparison of transfection efficiency using RB and HMB

To compare the effect of the microporation buffer in cell viability, recovery and overall yields, CGR8-NS cells were resuspended in RB or HMB and transfected with 2.0 x 10^{11} molecules of MC-GFP, pCMV-GFP and pVAX-eGFP (0.5 µg of MC-GFP and 0.8 µg of pCMV-GFP and VAX-eGFP), , using the fixed microporation settings for cells ressuspended in RB, 1500V/20ms/1pulse. Cells were analyzed after 24h for cell viability (data not shown) and recovery and percentage of GFP^+ cells (**Fig. 7**).

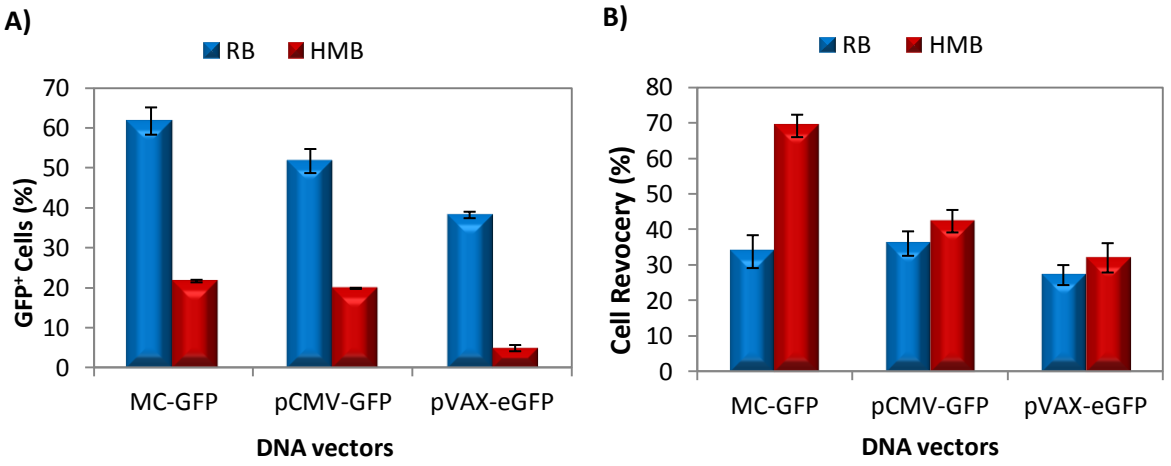

Figure 7: Comparison of Transfection efficiencies of CGR8-NSCs ressuspended in RB and HMB and transfected with different vectors (MC-GFP; pCMV-GFP; pVAX-eGFP) and transfected using 1500V/20ms/1p as microporation parameters.

CGR8-NSCs were transfected with 2.0 x 10^{11} molecules of MC-GFP, pCMV-GFP and pVAX-eGFP, and analyzed 24h after microporation **A)** Percentage of GFP^+ cells was assessed by flow cytometry and **B)** Cell Recovery was assessed by trypan blue staining. NM cells were used as controls (Control viability > 92%, not shown) and the results are expressed as mean ± SEM of four replicas of one experiment.

Slightly higher viabilities are achieved when using HMB as resuspension buffer (MC-GFP: ≈92%; pCMV-GFP: ≈87%; pVAX-eGFP: ≈87%) compared to cells resuspended in RB (MC-GFP: ≈91%; pCMV-GFP: ≈79%; pVAX-eGFP: ≈77%). The same pattern of results is obtained when evaluating cell recoveries of cells transfected with each vector. Cell recovery was higher for cells resuspended with HMB, regardless of the used vector (**Fig. 7B**), whereas, higher levels of GFP transfected cells were obtained when resuspending cells in RB, achieving a maximum of 62% for MC-GFP transfected cells, 52% for pCMV-GFP transfected cells and 38% for pVAX-eGFP transfected cells (**Fig. 7A**).

These results suggest that RB, a buffer of unknown composition, yields higher conductivity, and, as a consequence, might cause increased cellular death. On the other hand, the use of HMB as electroporation buffer, allows a more sustained survival of the cells, however, to achieve levels of GFP expression comparable to those obtained with RB, it is necessary to increase the voltage of the microporation conditions as it was evidenced by the obtained results with HMB and shown in section 4.4.2.

4.5. Effect of different gene vectors on NSC transgene expression

4.5.1. Long-term analysis of transfected cells

One of the major factors affecting non-viral gene transfer is the nature of the vector Therefore, to assess the effect of different gene vectors on CGR8-NS cells transgene expression, cells were transfected using different vectors, more specifically, MC-GFP, pCMV-GFP (both from Plasmid Factory) and pVAX-eGFP, which have different contents of CpG dinucleotides, that is, ~ 7% of pCMV-GFP and pVAX-eGFP backbone contain CpG motifs and ~ 6% of MC-GFP yield these dinucleotides (**Supplementary Table 1**).

To evaluate and compare cell proliferative capacity, maintenance and vector stability overtime, CGR8-NS cells were resuspended in RB and transfected with 2.0 x 10^{11} molecules of MC-GFP, pCMV-GFP and pVAX-eGFP using the optimized microporation conditions for RB, 1500V, 20 ms and 1 pulse. Cells were cultured for 10 days in 24-well plates and replated on day 4 to new 24-well plates when they reached confluence. The analysis was performed on days 1, 3, 4, 7 and 10 by trypan blue exclusion method and flow cytometry and on day 1 the cells were visualized by fluorescence microscopy.

Long term analysis showed that cells transfected with MC-GFP exhibit higher numbers of GFP expressing cells when compared to CGR8-NS cells transfected with pCMV-GFP and pVAX-eGFP. Among the three vectors the latter shows lower levels of GFP^+ cells. Nonetheless, cells transfected with MC-GFP and pCMV-GFP showed a similar profile, i.e., the number of cells expressing the transgene reached its maximum on day 3 (MC-GFP: ≈75%; pCMV-GFP: ≈ 58%) and slowly declined until day 10 where MC-GFP transfected cells still displayed 20% of GFP^+ cells compared to the 6% of GFP^+ cells exhibited by transfection with pCMV-GFP. On the other hand, transfection of CGR8-NS cells with pVAX-eGFP showed that the maximum of GFP^+ cells is achieved on day 1 (≈ 38%) and slowly declines until it almost ceases on day 10, where only 1% of the cells still express the transgene (**Fig. 8A**). The difference between both plasmids (pCMV-GFP and pVAX-eGFP) that might explain the differences in GFP expression relies on the GFP gene and most probably the sequence provided by plasmid factory gives rise to a brighter protein or encompass other sequences that increase gene expression levels.

The analysis of cell viabilities demonstrated that, when transfected, CGR8-NS cells are able to maintain a relatively stable survival rate. The results show that the highest cell viability levels were obtained upon MC-GFP transfection, which exhibit cell viability values of around 90% throughout the analyzed days, when compared with cells transfected with pCMV-GFP and pVAX-eGFP whose viabilities are maintained around 80% and 70% respectively. In pVAX-eGFP transfected cells, cell viability was only analyzed until day 4. On

day 4, due to culture confluence, a new passage was performed; however, the proliferation rate of transfected and non-transfected cells was probably influenced and by day 7, instead of adhering to the plate floor, the cells formed neurospheres. While MC-GFP and pCMV-GFP transfected CGR8-NSCs recovered, the ones transfected with pVAX-eGFP were not able to recuperate and culture was only maintained until this day (**Fig. 8B**).

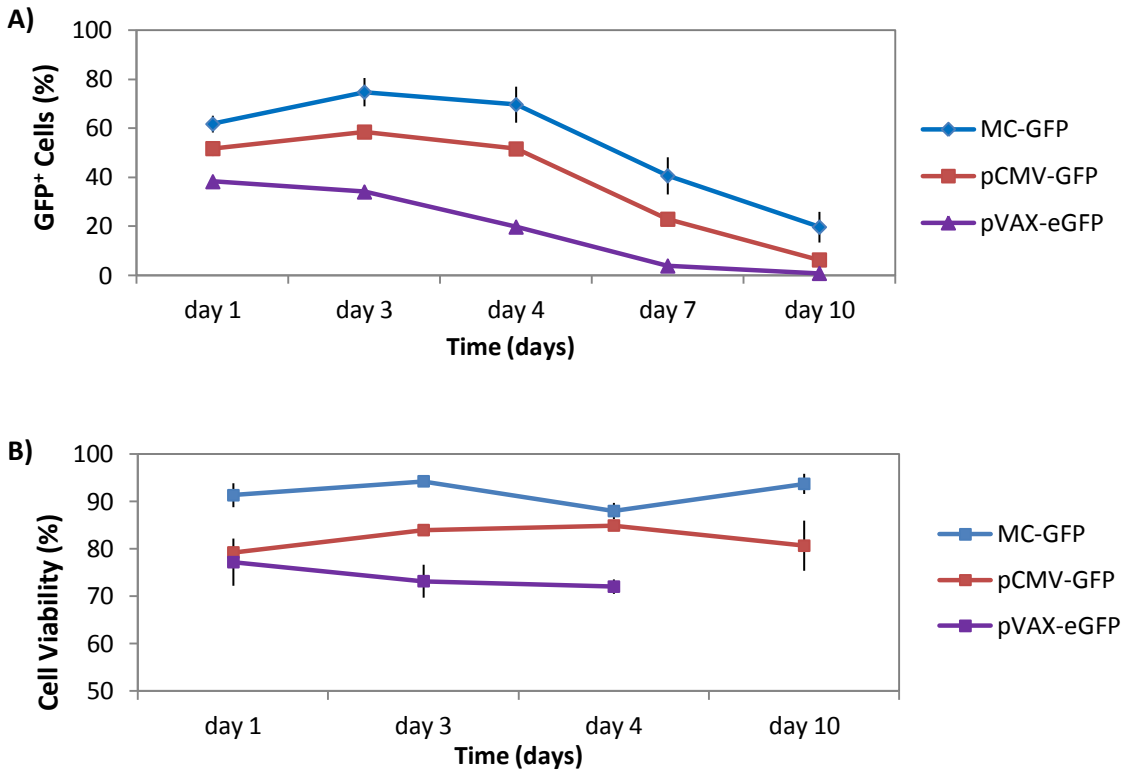

Figure 8: Long-term analysis of transfected CGR8-NSC for 10 days.

CGR8-NSCs were ressuspended in RB and transfected with 2.0 x 10^{11} molecules of MC-GFP, pCMV-GFP and pVAX-eGFP using 1500V/20ms/1p as microporation conditions. Cells were analyzed on days 1, 3, 4, 7 and 10 after microporation. **A)** Percentage of GFP expressing cells was assessed by flow cytometry and **B)** Cell Viability was assessed through trypan blue assay. NM cells were used as controls (Control viability from 91 to 97%) and the results are expressed as mean ± SEM of two independent experiments.

The fluorescence images obtained after 24h of transfection show that MC-GFP enables efficient gene delivery to CGR8-NS cells, displaying a high number of fluorescent cells and fluorescence intensity, without affecting their morphology that maintained their characteristic bipolar form (**Supplementary Fig. 4A and B**). In comparison, CGR8-NS cells transfected with pCMV-GFP (**Supplementary Fig.4C and D**) and pVAX-eGFP (**Supplementary Fig. 4E and F**) exhibit lower levels of transfection and transgene expression evidenced by the lower number of cells that display high fluorescence intensity. By the images it is also evident that although pCMV-GFP transfected cells maintain bipolar morphology, transfection with pVAX-eGFP impairs the survival rate and morphological characteristics of CGR8-NS cells. When compared to the others, these cells are smaller and rounder and present in a much lower number, hinting that their recovery rate is much slower.

Overall, these results indicate that gene delivery is most efficient when using MC-GFP as a delivery vector. Upon transfection with this vector it is possible to achieve high transgene expression without compromising their survival and morphology and for a longer period of time when compared with transfection with pCMV-GFP and pVAX-eGFP. Another relevant point is the difference found in expression levels and cell viability of pCMV-GFP and pVAX-eGFP transfected cells. Both vectors are plasmids with similar CpG content therefore the discrepancy found between the two vectors might be explained by the level of purification of both plasmids. Indeed the method of purification of pCMV-GFP accomplished by Plasmid Factory, might be more efficient than the Endotoxine Purification protocol used in-house to purify pVAX-eGFP.

4.5.2. Cell division kinetics analysis of transfected cells

To analyze the effect of each vector (MC-GFP, pCMV-GFP and pVAX-eGFP) on CGR8-NSC proliferation rate, cells were labeled with PKH67 and then transfected with 2.0 x 10^{11} molecules of each vector using 1500V, 20 ms and 1 pulse as microporation settings and cultured for 7 days. Non-microporated cells and transfected cells were then compared in terms of their cell division kinetics by flow cytometry.

Non-microporated cells and transfected cells showed a similar division profile on days 1, 3 and 7, independently of the used vector. On day 3 all the cells had undergone cell division and there weren't already any nondividing cells (Parent) present in culture. On the other hand, on day 4, while MC-GFP and pCMV-GFP transfected cells showed a division rate similar to the one of non-microporated cells, displaying most of the cells at Generation 4 (**Fig. 9A, B and C),** pVAX-eGFP transfected CGR8-NSC showed a small delay on cellular division exhibiting most of the cells evenly distributed at Generation 3 (≈ 39%) and 4 (≈ 36%)(**Fig. 9D**). By day 7, regardless of the vector, transfected cells were distributed around Generation 3 and 8 in rates similar to the ones found in the controls, an effect that might be due to the performed passage of the cells on day 4, which might have affected the proliferation rates of both transfected and non-transfected CGR8-NSC. These results suggest that, in CGR8-NSCs, the proliferation kinetics is not influenced upon transfection with MC-GFP and pCMV-GFP, but a slight delay appears when transfecting with pVAX-eGFP.

The comparison of the demonstrated proliferations with the transfection efficiencies of each vector show that, despite exhibiting higher numbers of cells presenting GFP fluorescence, the proliferation kinetics of cells transfected with MC-GFP and pCMV-GFP was not affected, even on days 3 and 4, when transgene expression reached its peak. Conversely, upon transfection with pVAX-eGFP a small delay in the division kinetics was detected even when the number of GFP expressing cells was declining. These combined

results suggest that, unlike MC-GFP and pCMV-GFP, the use of pVAX-eGFP as transgene vector might cause a slight alteration of the division rate of CGR8-NS cells.

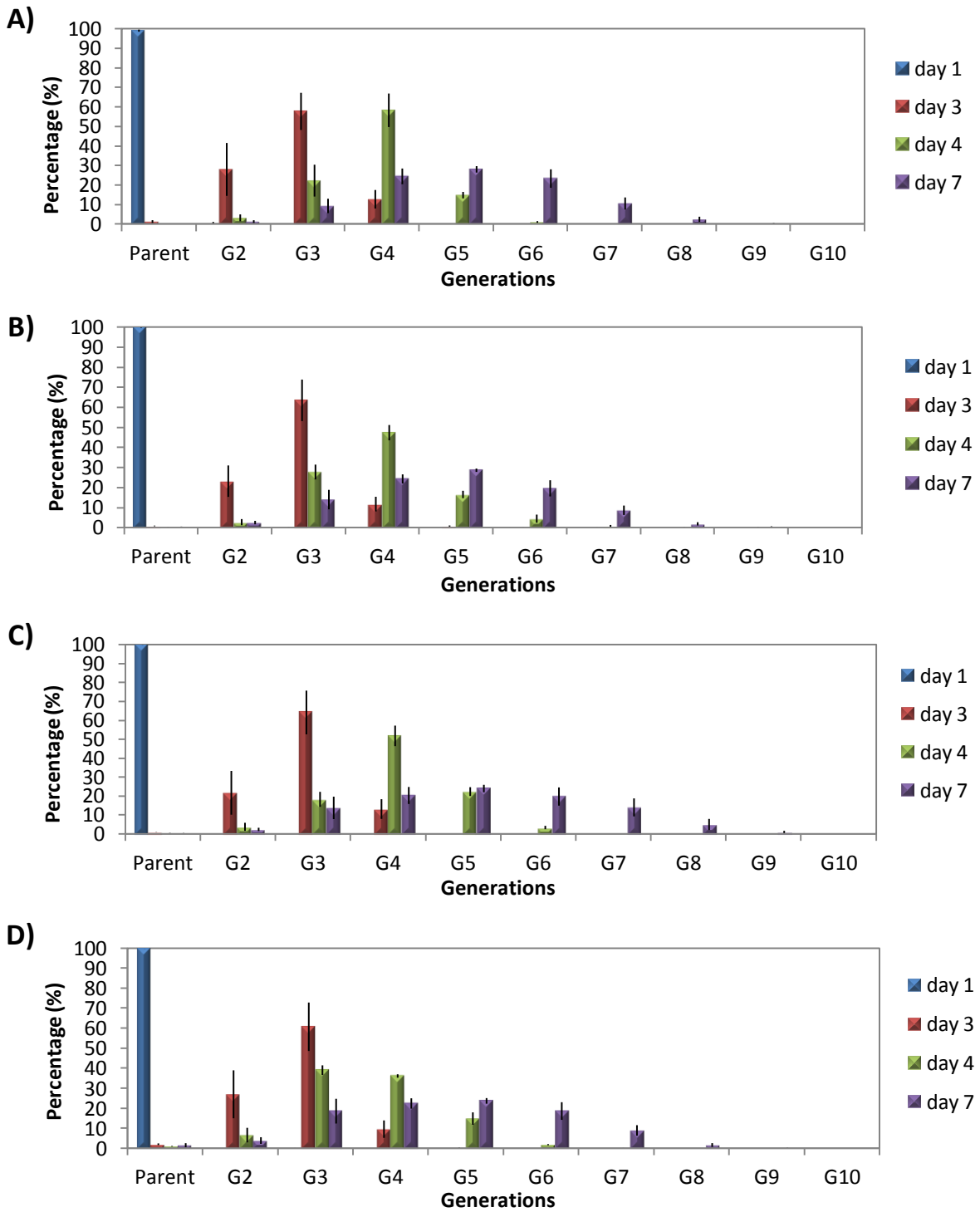

Figure 9: Cell division kinetics of transfected CGR8-NSC for 7 days.

CGR8-NSCs were labeled with PKH67 and data was acquired by flow cytometry at days 1, 3, 4 and 7. Each bar represents the percentage of cell in each doubling generation, along 7 days. **A)** Non-microporated cells; **B)** Cells transfected with MC-GFP; **C)** Cells transfected with pCMV-GFP; **D)** Cells transfected with pVAX-eGFP. Results are expressed as mean ± SEM of two independent assays.

4.6. Quantification of plasmid and minicircle copies in the nucleus

4.6.1. Calibration curves

To determine the number of plasmid and minicircle copies in the nucleus a standard curve for each vector was generated by spiking 20,000 of non-microporated CGR8-NSC with increasing amounts of vector DNA. A linear working range covering from 3 (61 molecules MC-GFP/cell; 39 molecules pCMV-GFP/cell; 37 molecules pVAX-eGFP/cell) to 30,000 pg (6.1 x 10^5 molecules MC-GFP/cell; 3.9 x 10^5 molecules pCMV-GFP; 3.7 x 10^5 molecules pVAX-eGFP/cell) was obtained for each vector (**Fig 10**). These curves allow the quantification of vector DNA in the nucleus and the obtained C_T of a sample corresponds to a determined number of copies.

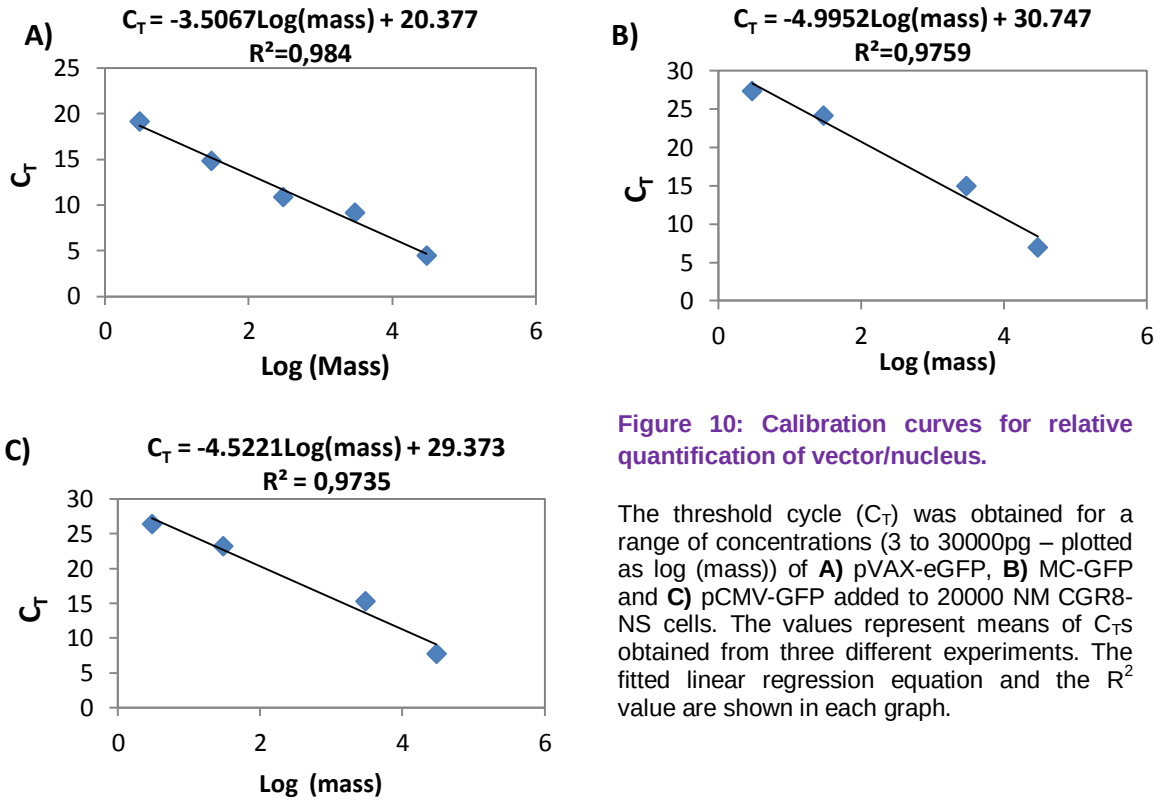

Figure 10: Calibration curves for relative quantification of vector/nucleus.

The threshold cycle (C_T) was obtained for a range of concentrations (3 to 30000pg – plotted as log (mass)) of **A)** pVAX-eGFP, **B)** MC-GFP and **C)** pCMV-GFP added to 20000 NM CGR8-NS cells. The values represent means of C_Ts obtained from three different experiments. The fitted linear regression equation and the R^2 value are shown in each graph.

4.6.2. DNA vector amount vs. gene expression

Nuclear uptake of vector DNA is usually impaired by extra- and intracellular barriers and is highly influenced by the type of used vector and delivery method, therefore, the obtained transgene expression is never a result of the whole amount of transfected vector copies. To determine the optimal dose of vector DNA from which transgene expression achieves its maximum level, CGR8-NS cells were resuspended in HMB and transfected with increasing amounts of vector DNA (0.1, 0.5, 0.8, 1.0 and 1.5 µg of MC-GFP, pCMV-GFP and pVAX-eGFP). Cells were analyzed after 24h by trypan blue exclusion method and flow cytometry and the number of vector DNA copies that reached the nucleus was determined using a standardized quantitative PCR (qPCR) assay.

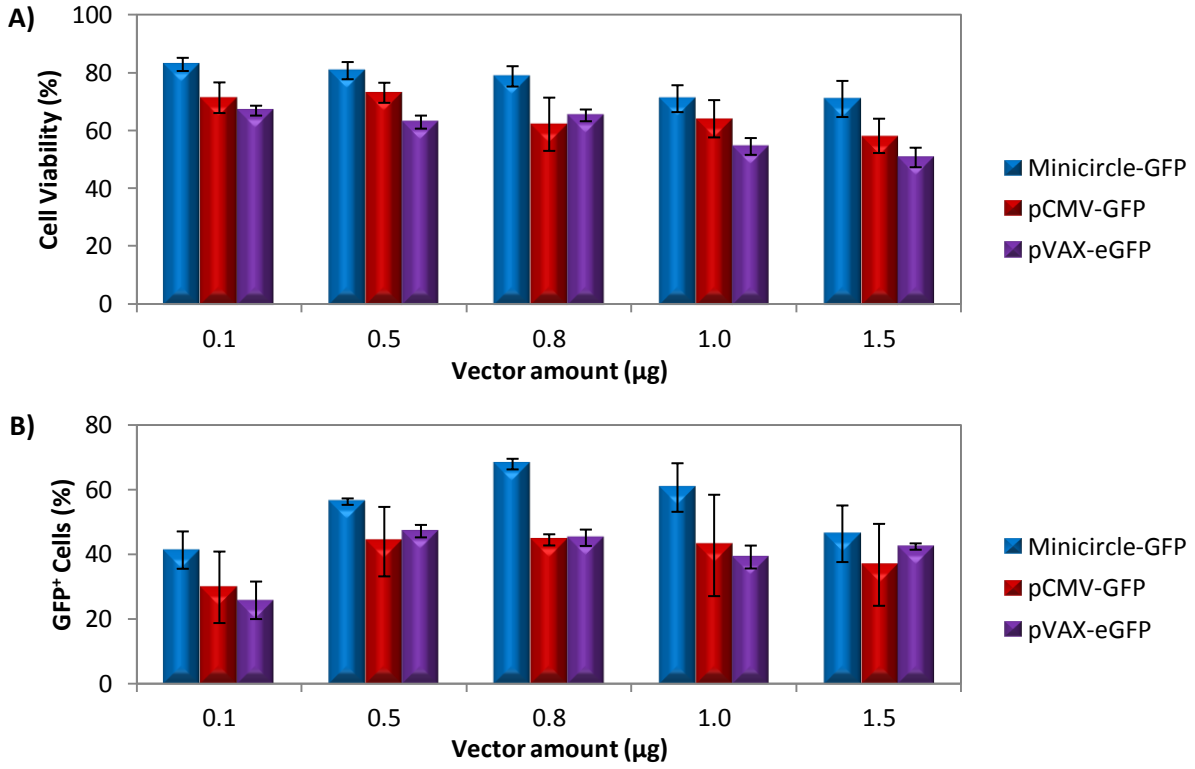

Figure 11: Transfection of CGR8-NS with different amounts of vector DNA.

CGR8-NSCs were ressuspended in HMB and transfected with 0.1, 0.5, 0.8, 1.0 and 1.5 µg of vector DNA (MC-GFP; pCMV-GFP; pVAX-eGFP). Cells were analyzed after 24h and A) Cell Viability was assessed by trypan blue exclusion method and B) % GFP^+ cells was obtained by flow cytometry analysis. NM cells were used as controls (Control viability ≈ 84%, not shown) and results are expressed as mean ±SEM of three independent experiments.

Once again, the results show that the highest number of transfected cells and cell viability are obtained upon transfection with MC-GFP (**Fig. 11**). Common to all the used vectors is the fact that cell viability slowly decreases with the increase of the DNA amount, ranging from 83 to 71%, 72 to 58% and 66 to 51% in MC-GFP, pCMV-GFP and pVAX-eGFP transfected cells respectively (**Fig.11A**), and, as depicted from **Fig. 11B**, transfection with 0.8 µg of MC-GFP, pCMV-GFP and pVAX-eGFP result in 68, 44 and 45% of GFP^+ cells

respectively, suggesting that the DNA amount which gives rise to the highest number of GFP expressing cells is 0.8 µg.

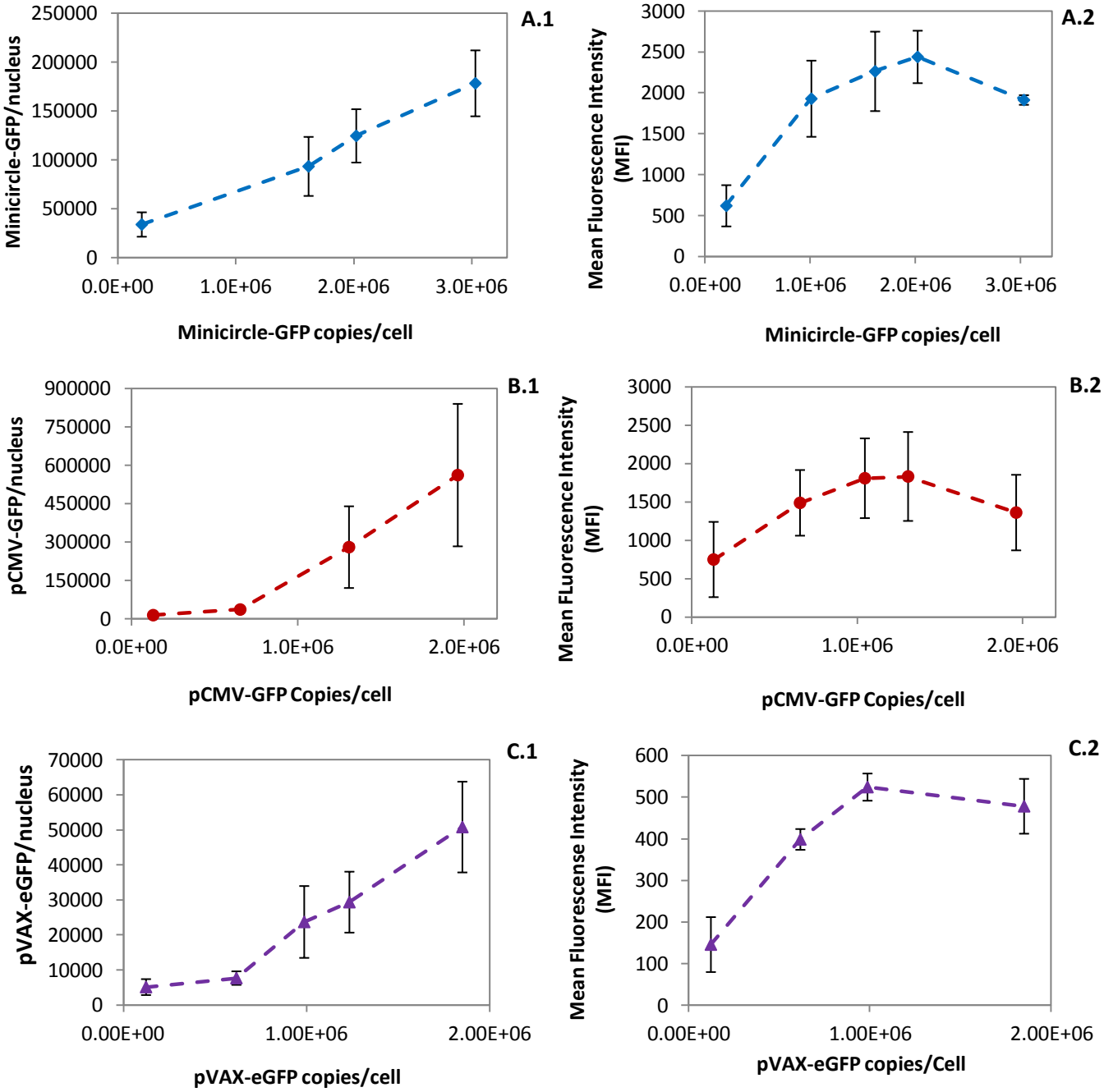

Figure 12: Quantification of vector DNA/nucleus and GFP expression intensity of CGR8-NS cells transfected with different amounts of vector DNA.

CGR8-NSCs were ressuspended in HMB and transfected with 0.1, 0.5, 0.8, 1.0 and 1.5 µg of each vector and analyzed after 24h. The quantification of **A.1)** MC-GFP, **B.1)** pCMV-GFP and **C.1)** pVAX-eGFP inside each nucleus was assessed by RT-PCR and the Mean Fluorescence Intensity (MFI) of **A.2**) MC-GFP, **B.2)** pCMV-GFP and **C.2)** pVAX-eGFP was determined through flow cytometry. NM cells were used as controls and the results are expressed as mean ± SEM of three independent assays.

In comparison, the quantification of vector DNA in the nucleus showed that, regardless of the vector, the number of copies inside the nucleus increase with the augment

of DNA amount. Cells transfected with MC-GFP, pCMV-GFP and pVAX-eGFP exhibited an increase from 34,000 to 178,000, 14,000 to 560,000 and 5,100 to 51,000 copies of vector DNA/ cell respectively (**Fig. 12A.1,B.1 and C.1**). On the other hand, when comparing with the MFI values it is clear that the increase in nuclear uptake of vector DNA is not correlated with the transcription of each transgene, indicating that, although the number of copies/nucleus increases with the amount of DNA, the expression of these vectors stabilize and eventually decrease with the highest amounts of provided DNA (**Fig. 12A.2, B.2 and C.2**). The differences between nuclear uptake of each vector DNA and GFP expression can be confirmed by the transfection of CGR8-NS cells with the lowest amounts of DNA, (from 2.02 x 10^5 to 1.62 x 10^6 copies of MC-GFP, 1.31 x 10^5 to 6.54 x 10^5 copies of pCMV-GFP and 1.23 x 10^5 to 9.87x10^5 copies of pVAX-eGFP per cell) which showed that the percentage of vector DNA that enters the nucleus is similar when using MC-GFP and pCMV-GFP as transfection vectors (around 10% using the lowest amount of DNA) , and lower upon pVAX-eGFP usage (around 4% with the lowest amount of DNA) (**Table 2**), however, the highest expression levels are obtained with MC-GFP that show MFI values ranging from 660 to 2265, when compared to pCMV-GFP and pVAX-eGFP whose values range from 746 to 1484 and 145 to 524 respectively (**Fig. 12A.2, B.2 and C.2**). For the highest amounts of pCMV-GFP, the obtained results showed higher percentages of nuclear uptake of this plasmid (**Table 2, Fig. 12B.1**), however, the obtained SEM values are also very high therefore further experiments need to be performed to confirm or refute the obtained results.

Table 2: Percentage of vector DNA inside the nucleus of CGR8-NS cells transfected with different amounts of MC-GFP, pCMV-GFP and pVAX-eGFP (results are expressed as Mean ± SEM of 3 independent experiments).

	Dose of vector/cell		% DNA inside the nucleus after 24 h (± SEM)
	No. Molecules	Mass (µg)	
Minicircle-GFP	2.02E+05	0.1	10.82 ± 4.79
	1.62E+06	0.8	5.78 ± 1.87
	2.02E+06	1.0	6.17 ± 1.35
	3.03E+06	1.5	5.89 ± 1.11
pCMV-GFP	1.31E+05	0.1	10.37 ± 2.66
	6.54E+05	0.5	5.44 ± 1.49
	1.31E+06	1.0	21.36 ± 12.21
	1.96E+06	1.5	28.59 ± 14.19
pVAX-eGFP	1.23E+05	0.1	4.14 ± 1.84
	6.17E+05	0.5	1.24 ± 0.31
	9.87E+05	0.8	2.40 ± 1.04
	1.23E+06	1.0	2.38 ± 0.71
	1.85E+06	1.5	2.75 ± 0.70

Altogether, these results suggest that saturation in transgene expression in CGR8-NS cells is achieved upon transfection with around 0.8 µg of vector DNA and that MC-GFP is the vector that is more efficiently expressed and the one that less affects cell survival. A comparison of the data obtained for MC-GFP and pCMV-GFP indicate that the highest percentage of CpG motifs in the latter might be the main factor affecting transgene expression which can be translated as a silencing triggered by the recognition of CpG motifs and posterior degradation of the plasmids.

4.6.3. Dilution kinetics of DNA vector along cell division

Dilution kinetics of vector DNA was assessed by quantifying overtime the number of vector copies present inside the nucleus of transfected cells. For this purpose CGR8-NS cells were resuspended in HMB and transfected with 2.0 x 10^{11} molecules of each vector using 1800V, 20 ms and 1 pulse as microporation conditions. Cells were cultured for 10 days and passaged on days 4 and 7 and analyzed at different points in time after transfection by trypan blue assay, flow cytometry and by quantification of vector copies in the nucleus was assessed by qPCR.

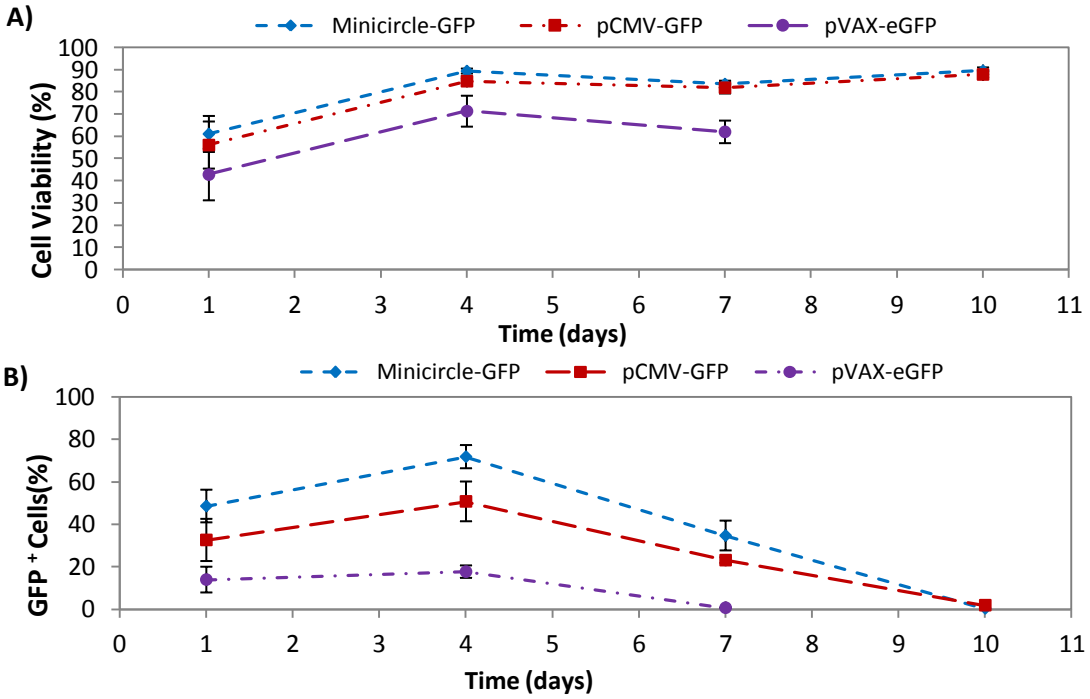

Figure 13: Long-term analysis of transfected CGR8-NS cells, using HMB along 10 days.

CGR8-NSCs were ressuspended in HMB and transfected with 2.0 x 10^{11} molecules of MC-GFP, pCMV-GFP and pVAX-eGFP and analyzed on days 1, 4, 7 and 10. **A)** Cell viability was assessed by trypan blue staining and **B)** Percentage of GFP^+ cells was assessed by flow cytometry analysis. NM cells were used as controls and the results are expressed as mean ± SEM of three independent experiments.

With the obtained results it's possible to compare the transfection efficiency of cells resuspended in HMB and RB overtime. Common to both experiments is that MC-GFP is the

vector that exhibits the highest cell viability values and the one that gives rise to the highest percentage of GFP^+ cells, however, when using HMB as electroporation buffer, there are some differences related to the initial values of cell viability and in the GFP expression decay throughout the analyzed days. Due to the fact that, to obtain higher number of GFP^+ cells microporation needs to be performed with higher voltages, the initial cell viability is lower (MC-GFP ≈61%, pCMV-GFP ≈56%, pVAX-eGFP ≈43%) when compared to the one obtained with RB (section 4.5.1, **Fig. 8**), however, it slowly increases (MC-GFP from 61 to 89%, pCMV-GFP from 56 to 88% and pVAX-eGFP from 43 to 70%) with the decrease of GFP expression levels (**Fig. 13A**). Moreover, although the percentage of GFP^+ cells decay profile is similar to the one obtained in the previously described long-term experiment, the obtained values are similar at first but decrease faster. For example, while in the first long-term experiment, on day 10 MC-GFP transfected cells still exhibited 20% of GFP^+ cells, in this experiment, by day 10 the number of GFP^+ cells is almost inexistent (**Fig. 13B**).

The level of GFP expression was also correlated with the number of vector copies/cell (**Table 3**). On day 1, after transfection there was a higher number of pCMV-GFP copies inside the nucleus (pCMV-CMV/cell = 195901) when compared to the other vectors. In comparison the number of copies/nucleus of MC-GFP transfected cells was slightly lower (MC-GFP/cell = 146414) and significantly lower in pVAX-eGFP transfected cells (pVAX-eGFP/cell = 12036). On the other hand, when comparing the MFI values on the first day, it is evident that even though less copies of MC-GFP were detected per nucleus, the expression levels are higher upon transfection with this vector. The analysis of the number of vector copies/nucleus on the other days show that MC-GFP dilution upon cell division is lower than the pDNAs and by day 4 and 7, the number of MC-GFP copies/nucleus and the transgene expression level is much higher when compared to the other vectors (**Table 3**), indicating that MC-GFP is the vector that persists more time inside the nucleus thus allowing a more sustained expression.

Table 3: Long-term quantification of vector DNA/nucleus and GFP expression intensity of CGR8-NS cells transfected with MC-GFP, pCMV-GFP and pVAX-eGFP (results are expressed as Mean ± SEM of 3 independent experiments).

	Minicircle-GFP		pCMV-GFP		pVAX-eGFP	
Time (days)	**MFI**	**Vector/cell**	**MFI**	**Vector/cell**	**MFI**	**Vector/cell**
1	1808 ± 232	146414 ± 20776	1089 ± 217	195901 ± 98823	163 ± 62	12036 ± 368
4	606 ± 249	11809 ± 1301	455 ± 113	1845 ± 1018	45 ± 12	1403 ± 1099
7	100 ± 42	2802 ± 1168	47 ± 8	321 ± 277	1,60 ± 1	123 ± 106

4.7. Differentiation of NSC

The differentiation potential of CGR8-NS cells into neurons after transfection was assessed by resuspending cells in HMB and transfecting them with 2.0 x 10^{11} molecules of pVAX-eGFP using 1800V, 20 ms and 1 pulse as microporation conditions. For neuronal differentiation non-microporated cells (**Fig. 14A**), microporated cells without DNA (**Fig. 14B**) and transfected cells (**Fig. 14C**) were submitted to the protocol described by Spiliotopoulos *et al* [31] and the result was determined by labeling of the neuronal marker Tuj1 (**Fig.14**; green labeling, white arrows). Both microporation (without DNA) and transfection with pVAX-eGFP did not seem to affect the CGR8-NSCs ability to differentiate into neurons; however, not many cells underwent differentiation, as it is shown by the low intensity of Tuj1 labeling. The difficulty in controlling the cell number after transfection, an essential factor in the neuralization protocol, might be the cause of this effect; therefore further experiments need to be performed to confirm the obtained results.

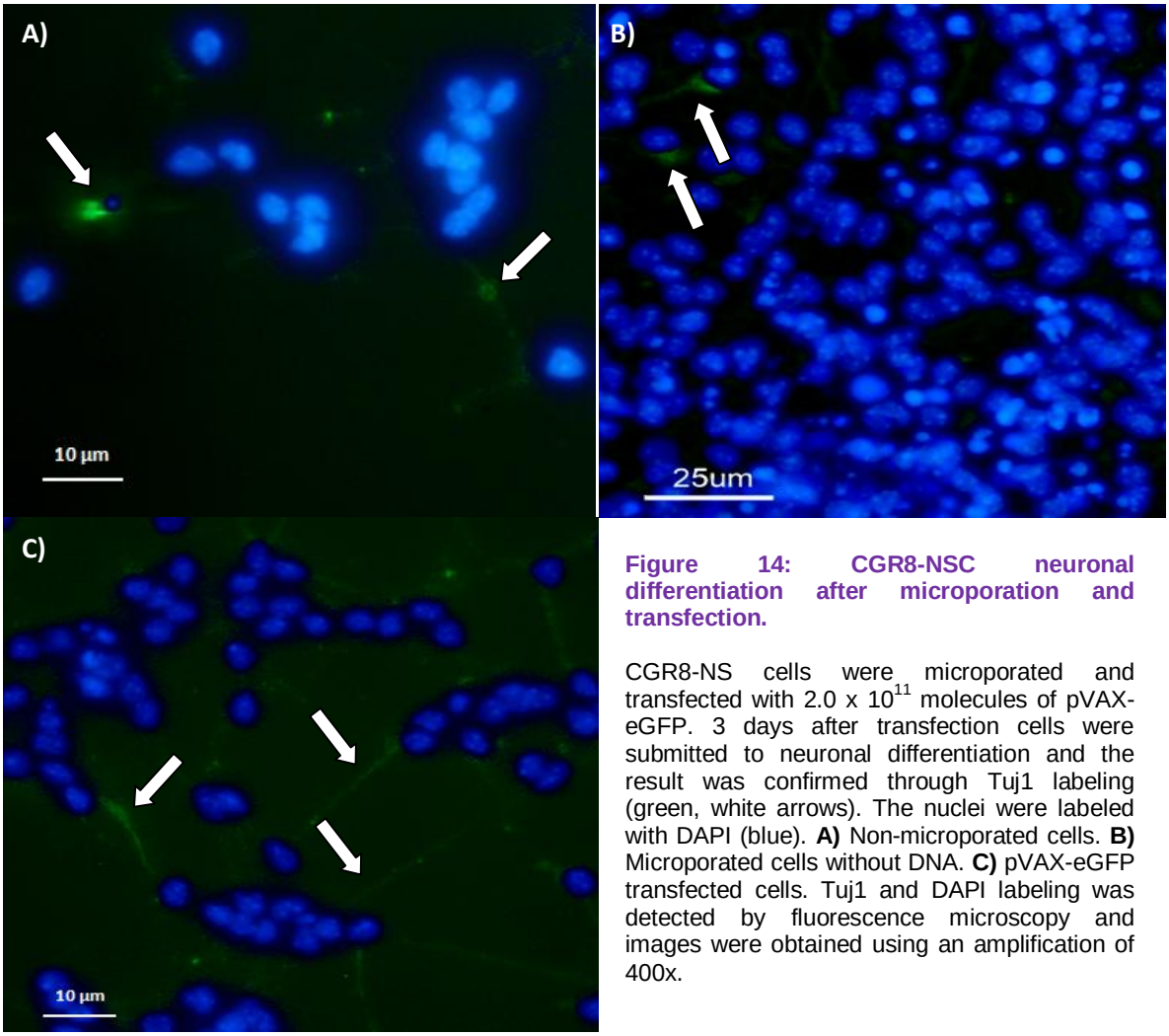

Figure 14: CGR8-NSC neuronal differentiation after microporation and transfection.

CGR8-NS cells were microporated and transfected with 2.0 x 10^{11} molecules of pVAX-eGFP. 3 days after transfection cells were submitted to neuronal differentiation and the result was confirmed through Tuj1 labeling (green, white arrows). The nuclei were labeled with DAPI (blue). **A)** Non-microporated cells. **B)** Microporated cells without DNA. **C)** pVAX-eGFP transfected cells. Tuj1 and DAPI labeling was detected by fluorescence microscopy and images were obtained using an amplification of 400x.

5. Discussion

In the past few years, NSCs have been the subject of intensive study to understand their biology and clinical application potential. Due to their proliferative capacity, relatively easy isolation and differentiation potential *in vitro*, NSCs have been considered an excellent resource for regeneration and gene therapies, therefore, their putative use for the treatment of neurological diseases, such as, neurodegenerative disorders and brain cancer, attract the interest of scientists all over the world. One of the major hurdles so far, has been the development of efficient gene delivery techniques that can be used for clinical applications. These methods, of viral and non-viral origin, often have some drawbacks either related to the type of used vector or the low transfection efficiencies obtained. For genetic manipulation, and future clinical application, it seems that the use of non-viral methods is preferable, yet, the low and transient transfection efficiencies usually obtained with these methods, cytotoxicity and maintenance of cell properties constitute the major setbacks for their future therapeutic application, therefore, to achieve the best results it is important to combine the best transfection technique with the best vector without neglecting the easy and safe handling that needs to be considered. However, it seems that the quest to find the perfect combination of method and vector is still in the beginning and the opinions about this matter vary worldwide.

In this study, in order to efficiently test the effect of different vectors in transfection of CGR8-NS cells, microporation conditions were optimized for the usage of two different electroporation buffers. Microporation is an efficient method that allows the obtainment of high transfection levels and cell viability and has proven to be efficient in transfection of several cell types [65-67]. However, being a recent developed technique to acquire the best results it is necessary to optimize the conditions in which the transfection of NSC will be performed. Transfection by microporation is usually impaired by voltage, pulse duration and number of pulses; nonetheless, the used electroporation buffer is also an important factor to take into account and, as recent reports showed, using cheaper buffers of known composition might result in good transfection efficiencies and improved survival [81-82]. For optimization of microporation conditions, CGR8-NS cells were resuspended in RB, a commercial electroporation buffer of unknown composition, provided by the equipment manufacturer, and HMB, a homemade electroporation buffer that was previously used in transfection of HEK293T cells and mesenchymal stem cells and proven to give rise to high transfection efficiencies and better cell viability values [65, 79].

When analyzing the obtained results it was possible to conclude that for transfection of CGR8-NS cells the preferred microporation condition, when using RB is 1500V, 20 ms and 1

pulse. With the first and second optimization assays, where voltage and pulse duration were tested, the highest transfection efficiency (≈60%) and cell viability and recovery (around 85-90%) values, and consequently, better yields of transfection (from 52 to 72%) were obtained upon transfection with 1500 V, 20 ms and 1 pulse. CGR8-NS cells proved to be resistant to high voltages, however, their survival, and as a consequence, the percentage of GFP^+ cells, was highly affected with the increase of pulse duration from 20 to 30 ms. In the third optimization assay using RB, the DNA amount was tested and optimized for transfection of CGR8-NS cells. Although the amount of DNA didn't seem to affect the number of GFP expressing cells (≈50%), higher cell recovery (≈86%) and yield of transfection (≈40%) was obtained when using 0.8 µg of pDNA. This fact is in agreement with the manufacturer instruction, and with recent reports which suggest the use of low amounts of DNA in microporation assays is more beneficial in terms of cell viability and consequently recovery and yield of transfection [65, 79].

When using HMB, to obtain high transfection efficiency values it was necessary to increase the voltage until 1800 V. In this condition it was able to achieve high numbers of GFP expressing cells, which, depending on the vector, varied from 58 to 75%, with a relative decrease of cell viability and recovery values (from 77 to 83% and 67 to 86%, depending on the vector), being the lower values the ones correspondent to the same vector used in optimization with RB. In fact, previous studies stated that there is a direct correlation with the increase of the voltage and transfection efficiency and cell death [83], therefore, as it can be seen from the obtained results, with the appropriate microporation condition it is possible to achieve high percentages of GFP expressing cells, however, the voltage increase might cause a slight decrease of the survival of the cells when using HMB.

In this study, the main objective was to test the effect of different vectors with distinct content of CpG dinucleotides on CGR8-NSCs transfection. When using a non-viral technique to transfect any type of cell, apart from the method, it is also important to wisely choose the ideal vector. These vectors are usually plasmids, that carry the gene of interest within an expression cassette that upon transfection is transcribed and translated [59]. The presence of unmethylated CpG dinucleotides in plasmid DNA can trigger immune responses thus increasing the risk of cytotxicity and impairing transgene expression. Once inside the cell, CpG motifs are recognized by TLR9. These receptors become activated and recruit the protein MyD88 that activates a signal cascade that leads to degradation of foreign DNA and the activation of innate and adaptive immune responses [84]. In NSCs the presence of TLR9 was not yet confirmed, however, the expression of many other Toll-Like receptors by aNSCs [85] suggest that their expression might be induced by the presence of bacterial CpG dinucleotides. The use of plasmids with reduced CpG content has shown to improve the

degree and persistence of gene expression and more recently, the use of CpGfree plasmids has demonstrated that upon *in vivo* transfection there is no activation of inflammatory responses and gene expression is sustained for more than 56 day [73]. When comparing the transfection efficiency of CGR8-NS cells transfected with CpGfree plasmids and pVAX-eGFP, a plasmid that has been shown to have improved resistance to the host nucleases hence allowing efficient transfection of CHO cells [1], it was evident that the pCpGfree was fast diluted and showed lower levels of gene expression. The commercial plasmid used for this testing was completely devoid of CpG motifs, however, for that purpose, all its sequences were either modified or newly synthesized, therefore, the problem with the levels and duration of transfection might be a consequence of this fact and, the modification of the promoter, which comprises a CMV enhancer, the EFI-a core promoter and a 5'-UTR containing a synthetic intron, and the polyA sequence, the late SV40 polyadenylation sequence, might be the factors responsible for this plasmid's weak performance.

Further experiments were performed with other vectors, such as the minicircle (2.2 Kb) and its correspondent plasmid, pCMV-GFP (3.5 Kb) and the results were compared with transfection with pVAX-eGFP (3.7 Kb). Minicircles are small vectors of plasmid origin that are completely devoid of bacterial sequences and therefore, have a lower content of CpG dinucleotides. These vectors represent a new alternative oh highly efficient and safe non-viral gene transfer and have been shown to induce a 10- to 10,000-fold improvement in the level and duration of gene expression [76-78]. In agreement with these data, the level of expression obtained with Minicircles in CGR8-NS cells was significantly higher, and more persistent when compared to its correspondent plasmid, pCMV-GFP, and also when compared with the other plasmid, the pVAX-eGFP. Significant differences were obtained among the three used vectors being the Minicircle the one that overall showed the better results, exhibiting an increase in GFP expression in the first 3 days reaching the maximum of 75% of GFP^+ cells with the maintenance of cell viability at around 90%. In contrast, although pCMV-GFP transfected cells showed the same decline in the percentage of GFP^+ cells, the values didn't go beyond 58% and cell viability was maintained at around 80%. Upon transfection with pVAX-eGFP the level of GFP expression reached its maximum (≈38%) on day 1, and cell viability values were maintained at around 70%. In comparison with the other plasmids which have around 7% of CpG dinucleotides in their constitution, the MC-GFP harbors only 6% of CpG dinucleotides and is smaller in size. It has been suggested that, upon transfection there is a size-dependent correlation with the mobility of the vector, indicating that, due to the presence of organelles that impose a high molecular crowding in the cytoplasm, the mobility of larger plasmids decrease making them more susceptible to degradation within the cell by the action of host nucleases [68-69]. Therefore, not only the

lack of bacterial backbone and low CpG content, but also the size of the minicircles might contribute to their improved performance, and in fact, recent studies demonstrated that reduced sized vectors contribute to enhanced gene expression level [Results from Ribeiro *et al*, under submission].

In terms of proliferation kinetics it seemed that the presence of minicircles and pCMV-GFP had no effect on cell division, while the presence of pVAX-eGFP seemed to slightly delay the proliferation on day 4 after transfection. These data could be also confirmed by the analysis of the morphology and cell numbers. Unlike minicircle and pCMV-GFP transfected cells, the ones transfected with pVAX-eGFP were present in small numbers and had a rounder morphology, and, when analyzing the overall cell viability, pVAX-eGFP transfected cells always showed the lower values, hinting that with the transfection, their survival and metabolism was affected. In previously described reports some authors have observed slowdown of cell growth and lower viabilities due to GFP expression and increased apoptosis due to the presence of pDNA [86-87], however, the obtained results indicate that NSCs might be resistant to transgene expression still, at some point they can be affected by the presence of plasmid DNA. In this case, since the slowdown was only detected in low rates with pVAX-eGFP, it can be concluded that NSCs biological response to pDNA transfection depends on the plasmid itself. As a matter of fact, recent studies demonstrated that upon transfection of the same gene with two different groups of plasmids significant differences were found in terms of cell apoptosis and consequently, cell viability [50]. Moreover, in this study and similarly to previous reports [50, 88], transfection didn't seem to affect NSCs ability to differentiate, and even after microporation with pVAX-eGFP, CGR8-NS cells specified into neurons.

In addition, uptake of vector copies by the nucleus was detected for CGR8-NS cells. Nuclear uptake of DNA vectors is usually affected by extra- and intracellular barriers; therefore, the obtained level of expression is never a translation of the entire supplied vector DNA. Recent studies showed that, although the nucleus can take large amounts of vector copies, only at low plasmid copy numbers gene expression can be correlated to the number of vector copies, and, there is a certain dose of vector after which the additional number of vector copies will not influence the level of transgene expression [89]. Recent reports determined that, depending on the used method and vector, only 1 to 10% of the delivered plasmids can be detected in the nuclei, and for example, in B16F10 mouse carcinoma cells and A549 human lung carcinoma cells, transfected with lipofectamine lipoplexes or polyethylenimine polyplexes, only 1 to 5% of the input DNA was detected in the nuclei [89-90]. With the quantification of intranuclear vectors it was possible to determine that the dose after which the transgene expression level stabilizes is around 0.8 µg of vector DNA.

Minicircles were the vectors that showed higher expression levels, even though in some cases fewer copies of minicircles were detected inside the nucleus. Moreover, long-term quantification showed that the minicircles are less degraded, exhibiting higher number of copies and GFP expression than pCMV-GFP and pVAX-eGFP transfected cells. These results demonstrate that the increase of just 1% of the CpG content in pCMV-GFP and pVAX-eGFP is enough to induce a faster and stronger inflammatory response by the cells after transfection thus leading to higher plasmid degradation and episomal transgene silencing.

The comparison of transfection efficiencies and number of GFP expressing cells show a big difference of values among the three tested vectors. The highest values were clearly obtained upon transfection with minicircles, however, even though pCMV-GFP and pVAX-eGFP have similar CpG content, there was a significant divergence in the results. The major differences between pVAX-eGFP and pCMV-GFP are the polyadenylation signal and the GFP gene. While MC-GFP and pCMV-GFP contain the SV40 polyA signal, pVAX-eGFP contains the BGH polyadenylation signal. Azzoni *et al* demonstrated that different polyA signals can give rise to differences in gene expression and that the efficiency of a vector depends not only on its ability to overcome physical and metabolic barriers but also on the effectiveness of regulatory sequences, such as, promoter and polyA sequence which are directly correlated with the mRNA frequency and half-life [1]. Recent studies show that transfection of hMSC with -SV40 vectors allows higher transfection efficiencies in comparison to –BGH vectors, while on hNSCs, better levels of GFP expressing cells are obtained with vectors with BGH [Results from Ribeiro *et al*, under submission]. Our results seem to contradict these data and suggest that –SV40 based vectors are more efficiently translated in NSCs than –BGH plasmids, showing higher levels of expression, however, in the experiments accomplished herein, besides polyadenylation signals the two plasmids encode different GFP genes being currently impossible to conclude about the main factor responsible for the observed differences in GFP expression. To further confirm or refute these results, additional studies of mRNA quantification need to be performed. Moreover these results might also be a result of the level of purification of each plasmid, hinting that pVAX-eGFP is more contaminated with bacterial DNA than pCMV-GFP and Minicircle-GFP.

Until recently, most of the gene delivery experiments to NSCs relied on the use of viral methods to efficiently transfect these cells, however, the problems often associated with these vectors are slowly shifting the researcher's attention to non-viral methodologies. Non-viral transfection of these cells has shown to be difficult and not very efficient. Dhara *et al* transfected NPs by nucleofection and obtained 37% of efficiency [91] while Sapet *et al,* using magnetofection with NeuroMag only achieved 15% of transfection efficiency [88].

Tinsley *et al* managed to transfect around 11, 16 and 20% of cells using FuGene6, ExGen500 and lipofectamine, respectively [92-93]. This study has demonstrated that combining an efficient non-viral method of transfection, such as microporation, with the most appropriate vector, a better transfection efficiency of NSCs is achieved. Vectors of low CpG content and smaller in size are more efficiently maintained inside the cell. This study shows that the use of Minicircles allows the obtainment of high transfection efficiencies, allowing the transfection of nearly 75% of the cells, without compromising cell survival and morphology, and, independently of the used transfection method, these vectors represent a very promising alternative for efficient gene delivery to Neural Stem Cells and a hope to the development of therapeutic applications for the treatment of neurodegenerative diseases or even brain cancer.

6. Conclusions and Future work

In this study gene delivery to NSCs was accomplished by microporation and the transfection efficiency was analyzed, under optimized conditions, for different types of vectors, more specifically, minicircles and plasmids with different CpG content. Up to date, there are no published data of microporation assays in NSCs and transfection of these cells with minicircles, therefore this study offers the first insights in the use of both technologies in non-viral transfection of NSCs. This study shows that non-viral transfection of NSCs by microporation constitutes an efficient method for gene delivery allowing the maintenance of the various cell traits and the obtainment of high expression levels. In conclusion this work demonstrates that the efficiency of non-viral gene delivery into NSCs can be increased by the use of small sized plasmids with low CpG content. In comparison with the other vectors, Minicircles showed improved transfection efficiency without compromising cell survival and morphology. Through the quantification of vector copies inside the nucleus it could be determined that the ideal dose of vector DNA to transfect NSCs is around 0.8 µg and it could be demonstrated that minicircles can be maintained inside the nucleus for longer periods of times and yield higher expression levels. Until recently one of the major problems related to minicircle technology was their production procedure, however, cheap and easy methods are being developed for large-scale production [74-75]. Altogether these results suggest that minicircles offer a new model of efficient and safe non-viral gene delivery to NSCs that can represent a desirable alternative for the development of therapies and clinical applications for the treatment of neurodegenerative diseases and brain cancer where a transient expression of the transgene might be necessary.

In terms of future work, to confirm if there is in reality an inflammatory response against CpG motifs it would be interesting to evaluate the expression of TLR9 of *in vitro* cultured NSCs after transfection with vectors of different CpG content. In order to evaluate the stability and frequency of transgene mRNA, it would also be interesting to quantify the number of mRNA copies after transfection with minicircles, pCMV-GFP and pVAX-eGFP and it would be beneficial to verify the efficiency of minicircles in gene delivery to NSCs using other transfection methods, such as Lipofection and Magnetofection. Additionaly, *in vivo* studies should be performed to evaluate the intracellular trafficking of minicircles.

Since this method is easy to handle and feasible, it would be interesting to clone minicircles with a gene of interest, such as BDNF or Shh, to direct gene induced neuronal differentiation [19-20], or others such as GDNF, VEGF and NGF or cytokines for *in vivo* testing of their effect in various neurodegenerative diseases, such as, Parkinson's disease, Alzheimer's disease or Spinal cord injury, and brain cancer.

7. References

1. Azzoni, A.R., S.C. Ribeiro, G.A. Monteiro, and D.M.F. Prazeres, *The impact of polyadenylation signals on plasmid nuclease-resistance and transgene expression.* The Journal of Gene Medicine, 2007. **9**(5): p. 392-402.
2. Moraleda, J.M., M. Blanquer, P. Bleda, P. Iniesta, F. Ruiz, S. Bonilla, C. Cabanes, L. Tabares, and S. Martinez, *Adult stem cell therapy: Dream or reality?* Transplant Immunology, 2006. **17**(1): p. 74-77.
3. Donovan, P.J.G., John, *The end of the beginning for pluripotent stem cells.* Nature Biotechnology, 2001. **414**(6859): p. 92-97.
4. Liu, N., M. Lu, X. Tian, and Z. Han, *Molecular mechanisms involved in self-renewal and pluripotency of embryonic stem cells.* Journal of Cellular Physiology, 2007. **211**(2): p. 279-286.
5. Knoepfler, P.S., *Deconstructing Stem Cell Tumorigenicity: A Roadmap to Safe Regenerative Medicine.* Stem Cells, 2009. **27**(5): p. 1050-1056.
6. Wagers, A.J. and I.L. Weissman, *Plasticity of Adult Stem Cells.* Cell, 2004. **116**(5): p. 639-648.
7. Brignier, A.C. and A.M. Gewirtz, *Embryonic and adult stem cell therapy.* The Journal of allergy and clinical immunology, 2010. **125**(2): p. S336-S344.
8. Conti, L. and E. Cattaneo, *Neural stem cell systems: physiological players or in vitro entities?* Nat Rev Neurosci, 2010. **11**(3): p. 176-187.
9. Okano, H., *Neural stem cells and strategies for the regeneration of the central nervous system.* Proceedings of the Japan Academy, Series B, 2010. **86**(4): p. 438-450.
10. Ying, Q.-L.S., Marios Griffiths, Dean Li, Meng Smith, Austin, *Conversion of embryonic stem cells into neuroectodermal precursors in adherent monoculture.* Nat Biotech, 2003. **21**(2): p. 183-186.
11. Pankratz, M.T., X.-J. Li, T.M. LaVaute, E.A. Lyons, X. Chen, and S.-C. Zhang, *Directed Neural Differentiation of Human Embryonic Stem Cells via an Obligated Primitive Anterior Stage.* Stem Cells, 2007. **25**(6): p. 1511-1520.
12. Bibel, M.R., Jens Schrenk, Katrin Tucker, Kerry Lee Staiger, Volker Korte, Martin Goetz, Magdalena Barde, Yves-Alain, *Differentiation of mouse embryonic stem cells into a defined neuronal lineage.* Nat Neurosci, 2004. **7**(9): p. 1003-1009.
13. Perrier, A.L., V. Tabar, T. Barberi, M.E. Rubio, J. Bruses, N. Topf, N.L. Harrison, and L. Studer, *Derivation of midbrain dopamine neurons from human embryonic stem cells.* Proceedings of the National Academy of Sciences of the United States of America, 2004. **101**(34): p. 12543-8.
14. Chambers, S.M., C.A. Fasano, E.P. Papapetrou, M. Tomishima, M. Sadelain, and L. Studer, *Highly efficient neural conversion of human ES and iPS cells by dual inhibition of SMAD signaling.* Nature Biotechnology, 2009. **27**(3): p. 275-80.
15. Yuan, S.H., J. Martin, J. Elia, J. Flippin, R.I. Paramban, M.P. Hefferan, J.G. Vidal, Y. Mu, R.L. Killian, M.A. Israel, N. Emre, S. Marsala, M. Marsala, F.H. Gage, L.S.B. Goldstein, and C.T. Carson, *Cell-Surface Marker Signatures for the Isolation of Neural Stem Cells, Glia and Neurons Derived from Human Pluripotent Stem Cells.* PLoS ONE, 2011. **6**(3): p. e17540.
16. Gonzalez-Perez, O., R. Romero-Rodriguez, M. Soriano-Navarro, J.M. Garcia-Verdugo, and A. Alvarez-Buylla, *Epidermal Growth Factor Induces the Progeny of Subventricular Zone Type B Cells to Migrate and Differentiate into Oligodendrocytes.* Stem Cells, 2009. **27**(8): p. 2032-2043.
17. Jackson, E.L., J.M. Garcia-Verdugo, S. Gil-Perotin, M. Roy, A. Quinones-Hinojosa, S. VandenBerg, and A. Alvarez-Buylla, *PDGFR±-Positive B Cells Are Neural Stem Cells in the Adult SVZ that Form Glioma-like Growths in Response to Increased PDGF Signaling.* Neuron, 2006. **51**(2): p. 187-199.
18. Kuhn, H.G., J. Winkler, G. Kempermann, L.J. Thal, and F.H. Gage, *Epidermal Growth Factor and Fibroblast Growth Factor-2 Have Different Effects on Neural Progenitors in the Adult Rat Brain.* The Journal of Neuroscience, 1997. **17**(15): p. 5820-5829.
19. Lai, K.K., Brian K. Gage, Fred H. Schaffer, David V. , *Sonic hedgehog regulates adult neural progenitor proliferation in vitro and in vivo.* Nat Neurosci, 2003. **6**(1): p. 21-27.
20. Galvao, R.P., J.M. Garcia-Verdugo, and A. Alvarez-Buylla, *Brain-derived neurotrophic factor signaling does not stimulate subventricular zone neurogenesis in adult mice and rats.* The Journal of neuroscience : the official journal of the Society for Neuroscience, 2008. **28**(50): p. 13368-83.
21. Battista, D., C.C. Ferrari, F.H. Gage, and F.J. Pitossi, *Neurogenic niche modulation by activated microglia: transforming growth factor β increases neurogenesis in the adult dentate gyrus.* European Journal of Neuroscience, 2006. **23**(1): p. 83-93.
22. Walton, N.M., B.M. Sutter, E.D. Laywell, L.H. Levkoff, S.M. Kearns, G.P. Marshall, B. Scheffler, and D.A. Steindler, *Microglia instruct subventricular zone neurogenesis.* Glia, 2006. **54**(8): p. 815-825.
23. Gonzalez-Perez, O., A. Quinones-Hinojosa, and J.M. Garcia-Verdugo, *Immunological control of adult neural stem cells.* Journal of stem cells, 2010. **5**(1): p. 23-31.
24. Kitchens, D.L., E.Y. Snyder, and D.I. Gottlieb, *FGF AND EGF ARE MITOGENS FOR IMMORTALIZED NEURAL PROGENITORS.* Journal of Neurobiology, 1994. **25**(7): p. 797-807.
25. Reynolds, B., W. Tetzlaff, and S. Weiss, *A multipotent EGF-responsive striatal embryonic progenitor cell produces neurons and astrocytes.* The Journal of Neuroscience, 1992. **12**(11): p. 4565-4574.
26. Campos, L.S., *Neurospheres: Insights into neural stem cell biology.* Journal of Neuroscience Research, 2004. **78**(6): p. 761-769.

27. Vukicevic, V., A. Jauch, T.C. Dinger, L. Gebauer, V. Hornich, S.R. Bornstein, M. Ehrhart-Bornstein, and A.M. Müller, *Genetic instability and diminished differentiation capacity in long-term cultured mouse neurosphere cells.* Mechanisms of Ageing and Development, 2010. **131**(2): p. 124-132.
28. Johe, K.K., T.G. Hazel, T. Muller, M.M. Dugich-Djordjevic, and R.D. McKay, *Single factors direct the differentiation of stem cells from the fetal and adult central nervous system.* Genes & Development, 1996. **10**(24): p. 3129-3140.
29. Conti, L., S.M. Pollard, T. Gorba, E. Reitano, M. Toselli, G. Biella, Y. Sun, S. Sanzone, Q.-L. Ying, E. Cattaneo, and A. Smith, *Niche-Independent Symmetrical Self-Renewal of a Mammalian Tissue Stem Cell.* PLoS Biol, 2005. **3**(9): p. e283.
30. Androutsellis-Theotokis, A., M.A. Rueger, D.M. Park, J.D. Boyd, R. Padmanabhan, L. Campanati, C.V. Stewart, Y. LeFranc, D. Plenz, S. Walbridge, R.R. Lonser, and R.D.G. McKay, *Angiogenic Factors Stimulate Growth of Adult Neural Stem Cells.* Plos One, 2010. **5**(2): p. e9414.
31. Spiliotopoulos, D., D. Goffredo, L. Conti, F. Di Febo, G. Biella, M. Toselli, and E. Cattaneo, *An optimized experimental strategy for efficient conversion of embryonic stem (ES)-derived mouse neural stem (NS) cells into a nearly homogeneous mature neuronal population.* Neurobiology of Disease, 2009. **34**(2): p. 320-331.
32. Sun, Y., S. Pollard, L. Conti, M. Toselli, G. Biella, G. Parkin, L. Willatt, A. Falk, E. Cattaneo, and A. Smith, *Long-term tripotent differentiation capacity of human neural stem (NS) cells in adherent culture.* Molecular and Cellular Neuroscience, 2008. **38**(2): p. 245-258.
33. Koch, P., T. Opitz, J.A. Steinbeck, J. Ladewig, and O. Brüstle, *A rosette-type, self-renewing human ES cell-derived neural stem cell with potential for in vitro instruction and synaptic integration.* Proceedings of the National Academy of Sciences, 2009. **106**(9): p. 3225-3230.
34. Pevny, L.H. and S.K. Nicolis, *Sox2 roles in neural stem cells.* The International Journal of Biochemistry & Cell Biology, 2010. **42**(3): p. 421-424.
35. Mo, Z. and N. Zecevic, *Is Pax6 Critical for Neurogenesis in the Human Fetal Brain?* Cerebral Cortex, 2008. **18**(6): p. 1455-1465.
36. Frederiksen, K. and R. McKay, *Proliferation and differentiation of rat neuroepithelial precursor cells in vivo.* The Journal of Neuroscience, 1988. **8**(4): p. 1144-1151.
37. Petit, A., A.D. Sanders, T.E. Kennedy, W. Tetzlaff, K.J. Glattfelder, R.A. Dalley, R.B. Puchalski, A.R. Jones, and A.J. Roskams, *Adult Spinal Cord Radial Glia Display a Unique Progenitor Phenotype.* Plos One, 2011. **6**(9): p. e24538.
38. Zhang, R., Z. Zhang, C. Zhang, L. Zhang, A. Robin, Y. Wang, M. Lu, and M. Chopp, *Stroke Transiently Increases Subventricular Zone Cell Division from Asymmetric to Symmetric and Increases Neuronal Differentiation in the Adult Rat.* The Journal of Neuroscience, 2004. **24**(25): p. 5810-5815.
39. Türeyen, K., R. Vemuganti, K.A. Sailor, K.K. Bowen, and R.J. Dempsey, *Transient focal cerebral ischemia—induced neurogenesis in the dentate gyrus of the adult mouse.* Journal of Neurosurgery, 2004. **101**(5): p. 799-805.
40. Martino, G.P., Stefano, *The therapeutic potential of neural stem cells.* Nat Rev Neurosci, 2006. **7**(5): p. 395-406.
41. Joers, V.L. and M.E. Emborg, *Preclinical assessment of stem cell therapies for neurological diseases.* ILAR journal / National Research Council, Institute of Laboratory Animal Resources, 2009. **51**(1): p. 24-41.
42. Dziewczapolski, G., D.C. Lie, J. Ray, F.H. Gage, and C.W. Shults, *Survival and differentiation of adult rat-derived neural progenitor cells transplanted to the striatum of hemiparkinsonian rats.* Experimental Neurology, 2003. **183**(2): p. 653-664.
43. Kelly, S., T.M. Bliss, A.K. Shah, G.H. Sun, M. Ma, W.C. Foo, J. Masel, M.A. Yenari, I.L. Weissman, N. Uchida, T. Palmer, and G.K. Steinberg, *Transplanted human fetal neural stem cells survive, migrate, and differentiate in ischemic rat cerebral cortex.* Proceedings of the National Academy of Sciences of the United States of America, 2004. **101**(32): p. 11839-11844.
44. Einstein, O., D. Karussis, N. Grigoriadis, R. Mizrachi-Kol, E. Reinhartz, O. Abramsky, and T. Ben-Hur, *Intraventricular transplantation of neural precursor cell spheres attenuates acute experimental allergic encephalomyelitis.* Molecular and Cellular Neuroscience, 2003. **24**(4): p. 1074-1082.
45. Behrstock, S., A. Ebert, J. McHugh, S. Vosberg, J. Moore, B. Schneider, E. Capowski, D. Hei, J. Kordower, P. Aebischer, and C.N. Svendsen, *Human neural progenitors deliver glial cell line-derived neurotrophic factor to parkinsonian rodents and aged primates.* Gene Therapy, 2006. **13**(5): p. 379-388.
46. Klein, S.M., S. Behrstock, J. McHugh, K. Hoffmann, K. Wallace, M. Suzuki, P. Aebischer, and C.N. Svendsen, *GDNF Delivery Using Human Neural Progenitor Cells in a Rat Model of ALS.* Human Gene Therapy, 2005. **16**(4): p. 509-521.
47. Tuszynski, M.H., L. Thal, M. Pay, D.P. Salmon, H.S. U, R. Bakay, P. Patel, A. Blesch, H.L. Vahlsing, G. Ho, G. Tong, S.G. Potkin, J. Fallon, L. Hansen, E.J. Mufson, J.H. Kordower, C. Gall, and J. Conner, *A phase 1 clinical trial of nerve growth factor gene therapy for Alzheimer disease.* Nat Med, 2005. **11**(5): p. 551-555.
48. Nagahara, A.H., D.A. Merrill, G. Coppola, S. Tsukada, B.E. Schroeder, G.M. Shaked, L. Wang, A. Blesch, A. Kim, J.M. Conner, E. Rockenstein, M.V. Chao, E.H. Koo, D. Geschwind, E. Masliah, A.A. Chiba, and M.H. Tuszynski, *Neuroprotective effects of brain-derived neurotrophic factor in rodent and primate models of Alzheimer's disease.* Nature Medicine, 2009. **15**(3): p. 331-7.

49. Kim, H.M., D.H. Hwang, J.E. Lee, S.U. Kim, and B.G. Kim, *<italic>Ex Vivo</italic> VEGF Delivery by Neural Stem Cells Enhances Proliferation of Glial Progenitors, Angiogenesis, and Tissue Sparing after Spinal Cord Injury.* Plos One, 2009. **4**(3): p. e4987.
50. Jin, H.L., W.A. Pennant, M. Hyung Lee, S.S. An, H.A. Kim, M.L. Liu, J.S. Oh, J. Cho, K.N. Kim, D.H. Yoon, and Y. Ha, *Neural Stem Cells Modified by a Hypoxia-Inducible VEGF Gene Expression System Improve Cell Viability under Hypoxic Conditions and Spinal Cord Injury.* Spine (Phila Pa 1976), 2010: p. 1-1.
51. Kim, S., *Neural Stem Cell-based Gene Therapy for Brain Tumors.* Stem Cell Reviews and Reports, 2011. **7**(1): p. 130-140.
52. Kay, M.A., J.C. Glorioso, and L. Naldini, *Viral vectors for gene therapy: the art of turning infectious agents into vehicles of therapeutics.* Nat Med, 2001. **7**(1): p. 33-40.
53. Jo, J.-i. and Y. Tabata, *Non-viral gene transfection technologies for genetic engineering of stem cells.* European Journal of Pharmaceutics and Biopharmaceutics, 2008. **68**(1): p. 90-104.
54. Hughes, S.M., F. Moussavi-Harami, S.L. Sauter, and B.L. Davidson, *Viral-mediated gene transfer to mouse primary neural progenitor cells.* Molecular Therapy, 2002. **5**(1): p. 16-24.
55. Donsante, A., D.G. Miller, Y. Li, C. Vogler, E.M. Brunt, D.W. Russell, and M.S. Sands, *AAV Vector Integration Sites in Mouse Hepatocellular Carcinoma.* Science, 2007. **317**(5837): p. 477.
56. Russell, D.W., *AAV Vectors, Insertional Mutagenesis, and Cancer.* Mol Ther, 2007. **15**(10): p. 1740-1743.
57. Jang, J.-H., J.T. Koerber, J.-S. Kim, P. Asuri, T. Vazin, M. Bartel, A. Keung, I. Kwon, K.I. Park, and D.V. Schaffer, *An Evolved Adeno-associated Viral Variant Enhances Gene Delivery and Gene Targeting in Neural Stem Cells.* Mol Ther, 2011. **19**(4): p. 667-675.
58. Latorre-Romero, C., M. Marin-Yaseli, C. Belmar-Lopez, R. del Moral, P. Marijuan, M. Quintanilla, and P. Martin-Duque, *Using living cells to transport therapeutic genes for cancer treatment.* Clinical and Translational Oncology, 2011. **13**(1): p. 10-17.
59. Kay, M.A., *State-of-the-art gene-based therapies: the road ahead.* Nat Rev Genet, 2011. **12**(5): p. 316-328.
60. Watanabe, S., A. Albsoul-Younes, T. Kawano, H. Itoh, Y. Kaziro, S. Nakajima, and Y. Nakajima, *Calcium phosphate-mediated transfection of primary cultured brain neurons using GFP expression as a marker: application for single neuron electrophysiology.* Neurosci Res, 1999. **33**: p. 71 - 78.
61. Luten, J., C.F. van Nostrum, S.C. De Smedt, and W.E. Hennink, *Biodegradable polymers as non-viral carriers for plasmid DNA delivery.* Journal of Controlled Release, 2008. **126**(2): p. 97-110.
62. Schleef, M., M. Blaesen, M. Schmeer, R. Baier, C. Marie, G. Dickson, and D. Scherman, *Production of Non Viral DNA Vectors.* Current Gene Therapy, 2010. **10**(6): p. 487-507.
63. Ino, K., T. Kawasumi, A. Ito, and H. Honda, *Plasmid DNA transfection using magnetite cationic liposomes for construction of multilayered gene-engineered cell sheet.* Biotechnology and Bioengineering, 2008. **100**(1): p. 168-176.
64. Kim, B.G., Y.M. Kang, J.H. Phi, Y.H. Kim, D.H. Hwang, J.Y. Choi, S. Ryu, A.E. Elastal, S.H. Paek, K.C. Wang, S.H. Lee, S.U. Kim, and B.W. Yoon, *Implantation of polymer scaffolds seeded with neural stem cells in a canine spinal cord injury model.* Cytotherapy. **12**(6): p. 841-845.
65. Madeira, C., S.C. Ribeiro, I.S.M. Pinheiro, S.A.M. Martins, P.Z. Andrade, C.L. da Silva, and J.M.S. Cabral, *Gene delivery to human bone marrow mesenchymal stem cells by microporation.* Journal of Biotechnology, 2011. **151**(1): p. 130-136.
66. Marucci, G., C. Lammi, M. Buccioni, D. Dal Ben, C. Lambertucci, C. Amantini, G. Santoni, M. Kandhavelu, M.P. Abbracchio, D. Lecca, R. Volpini, and G. Cristalli, *Comparison and optimization of transient transfection methods at human astrocytoma cell line 1321N1.* Analytical Biochemistry, 2011. **414**(2): p. 300-302.
67. Lim, J.Y., S.H. Park, C.H. Jeong, J.H. Oh, S.M. Kim, C.H. Ryu, S.A. Park, J.G. Ahn, W. Oh, S.S. Jeun, and J.W. Chang, *Microporation is a valuable transfection method for efficient gene delivery into human umbilical cord blood-derived mesenchymal stem cells.* Bmc Biotechnology. **10**.
68. Vaughan, E.E., J.V. DeGiulio, and D.A. Dean, *Intracellular Trafficking of Plasmids for Gene Therapy: Mechanisms of Cytoplasmic Movement and Nuclear Import.* Current Gene Therapy, 2006. **6**(6): p. 671-681.
69. Wiethoff, C.M. and C.R. Middaugh, *Barriers to nonviral gene delivery.* Journal of Pharmaceutical Sciences, 2003. **92**(2): p. 203-217.
70. Escoffre, J.-M., J. Teissié, and M.-P. Rols, *Gene Transfer: How Can the Biological Barriers Be Overcome?* Journal of Membrane Biology, 2010. **236**(1): p. 61-74.
71. Gill, D.R., I.A. Pringle, and S.C. Hyde, *Progress and Prospects: The design and production of plasmid vectors.* Gene Ther, 2009. **16**(2): p. 165-171.
72. Nishikawa, M., S. Rattanakiat, and Y. Takakura, *DNA-based nano-sized systems for pharmaceutical and biomedical applications.* Advanced Drug Delivery Reviews, 2010. **62**(6): p. 626-632.
73. Hyde, S.C., I.A. Pringle, S. Abdullah, A.E. Lawton, L.A. Davies, A. Varathalingam, G. Nunez-Alonso, A.M. Green, R.P. Bazzani, S.G. Sumner-Jones, M. Chan, H. Li, N.S. Yew, S.H. Cheng, A.C. Boyd, J.C. Davies, U. Griesenbach, D.J. Porteous, D.N. Sheppard, F.M. Munkonge, E. Alton, and D.R. Gill, *CpG-free plasmids confer reduced inflammation and sustained pulmonary gene expression.* Nature Biotechnology, 2008. **26**(5): p. 549-551.

74. Chen, Z.Y., C.Y. He, and M.A. Kay, *Improved production and purification of minicircle DNA vector free of plasmid bacterial sequences and capable of persistent transgene expression in vivo.* Human Gene Therapy, 2005. **16**(1): p. 126-131.
75. Kay, M.A., C.-Y. He, and Z.-Y. Chen, *A robust system for production of minicircle DNA vectors.* Nat Biotech, 2010. **28**(12): p. 1287-1289.
76. Chen, Z.-Y., C.-Y. He, A. Ehrhardt, and M.A. Kay, *Minicircle DNA Vectors Devoid of Bacterial DNA Result in Persistent and High-Level Transgene Expression in Vivo.* Mol Ther, 2003. **8**(3): p. 495-500.
77. Huang, M., Z. Chen, S. Hu, F. Jia, Z. Li, G. Hoyt, R.C. Robbins, M.A. Kay, and J.C. Wu, *Novel Minicircle Vector for Gene Therapy in Murine Myocardial Infarction.* Circulation, 2009. **120**(11 suppl 1): p. S230-S237.
78. Argyros, O., S. Wong, C. Fedonidis, O. Tolmachov, S. Waddington, S. Howe, M. Niceta, C. Coutelle, and R. Harbottle, *Development of S/MAR minicircles for enhanced and persistent transgene expression in the mouse liver.* Journal of Molecular Medicine, 2011. **89**(5): p. 515-529.
79. Madeira, C., S. Ribeiro, M. Turk, and J. Cabral, *Optimization of gene delivery to HEK293T cells by microporation using a central composite design methodology.* Biotechnology Letters, 2010. **32**(10): p. 1393-1399.
80. dos Santos, F., P.Z. Andrade, J.S. Boura, M.M. Abecasis, C.L. da Silva, and J.M.S. Cabral, *Ex vivo expansion of human mesenchymal stem cells: A more effective cell proliferation kinetics and metabolism under hypoxia.* Journal of Cellular Physiology, 2010. **223**(1): p. 27-35.
81. Kang, J., S. Ramu, S. Lee, B. Aguilar, S.K. Ganesan, J. Yoo, V.K. Kalra, C.J. Koh, and Y.-K. Hong, *Phosphate-buffered saline-based nucleofection of primary endothelial cells.* Analytical Biochemistry, 2009. **386**(2): p. 251-255.
82. Ferreira, E.P., E Logeart-Avramoglou, D Salomskaite-Davalgiene, S Mir, L M Petite, H, *Optimization of a gene electrotransfer method for mesenchymal stem cell transfection.* Gene Therapy, 2008. **15**(7): p. 537-544http://dx.doi.org/10.1038/gt.2008.9.
83. Gu, W.X.L.Z.Y.M.H., *Charged Magnetic nanoposrticles for enhancing gene transfection.* Nanotechnology, IEEE Transactions on, 2009. **8**(2): p. 142-147.
84. Wagner, H., *Toll Meets Bacterial CpG-DNA.* Immunity, 2001. **14**: p. 499-502.
85. Carpentier, P.A. and T.D. Palmer, *Immune Influence on Adult Neural Stem Cell Regulation and Function.* Neuron, 2009. **64**(1): p. 79-92.
86. Levetzow, G.V., J. Spanholtz, J. Beckmann, J. Fischer, G. Kögler, P. Wernet, M. Punzel, and B. Giebel, *Nucleofection, an Efficient Nonviral Method to Transfer Genes into Human Hematopoietic Stem and Progenitor Cells.* Stem Cells and Development, 2006. **15**(2): p. 278-285.
87. LI, L.H., P. MCCARTHY, and S.W. HUI, *High-efficiency electrotransfection of human primary hematopoietic stem cells.* The FASEB Journal, 2001. **15**(3): p. 586-588.
88. Sapet, C., Laurent, N., Chevigny, A., Le Gourrierec, L., Bertosio, E., Zelphati, O., Béclin, C., *High transfection efficiency of neural stem cells with magnetofection.* Biotechniques, 2011. **30**(3): p. 187-189.
89. Cohen, R.N., M.A.E.M. van der Aa, N. Macaraeg, A.P. Lee, and F.C. Szoka Jr, *Quantification of plasmid DNA copies in the nucleus after lipoplex and polyplex transfection.* Journal of Controlled Release, 2009. **135**(2): p. 166-174.
90. Lam, A.P.D., D A, *Progress and prospects: nuclear import of nonviral vectors.* Gene Therapy, 2011. **17**(4): p. 439-447.
91. Dhara, S.K., B.A. Gerwe, A. Majumder, M.C. Dodla, N.L. Boyd, D.W. Machacek, K. Hasneen, and S.L. Stice, *Genetic manipulation of neural progenitors derived from human embryonic stem cells.* Tissue engineering. Part A, 2009. **15**(11): p. 3621-34.
92. Tinsley, R.B., M.J. Vesey, S. Barati, R.A. Rush, and I.A. Ferguson, *Improved non-viral transfection of glial and adult neural stem cell lines and of primary astrocytes by combining agents with complementary modes of action.* The Journal of Gene Medicine, 2004. **6**(9): p. 1023-1032.
93. Tinsley, R.B., J. Faijerson, and P.S. Eriksson, *Efficient non-viral transfection of adult neural stem/progenitor cells, without affecting viability, proliferation or differentiation.* The Journal of Gene Medicine, 2006. **8**(1): p. 72-81.

Supplementary Figures

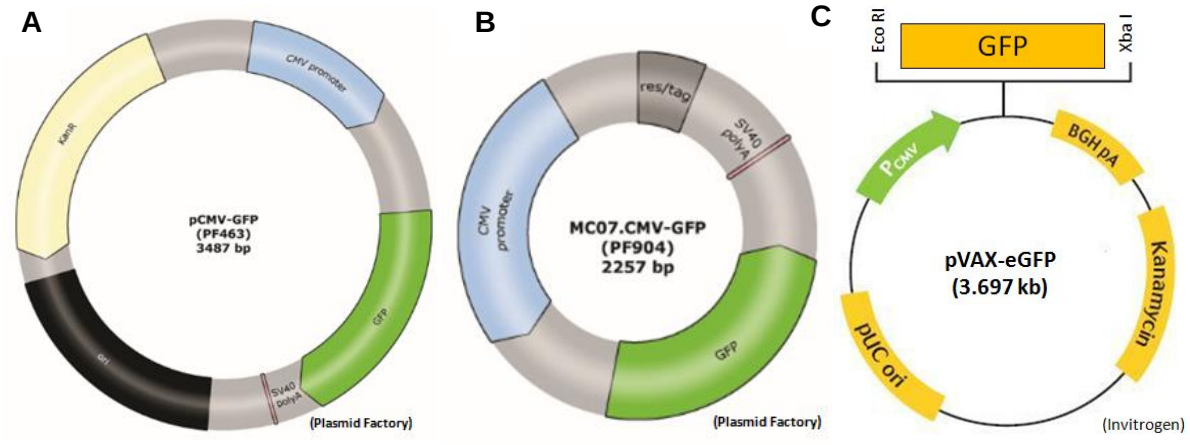

Supplementary Figure 1: Restriction maps of the commercial vectors pCMV-GFP and MC07.CMV-GFP (MC-GFP) and the pVAX-eGFP construction.

A) Restriction map of pCMV-GFP, consisting of: CMV enhancer/promoter; GFP sequence (Plasmid Factory); SV40 polyA signal; bacterial origin of replication (ori) and a Kanamycin resistance gene. **B)** Restriction map of MC07.CMV-GFP, consisting of: CMV promoter, GFP sequence (Plasmid Factory); SV40 polyaA signal and res/tag sequence (site-specific recombination sequence). **C)** Restriction map of the construction pVAX-eGFP consisting of: CMV promoter, Bovine growth hormone polyA signal (BGH pA); Kanamycin resistance gene; bacterial origin of replication (pUC) and eGFP sequence that was inserted as previously described by Azzoni *et al.*

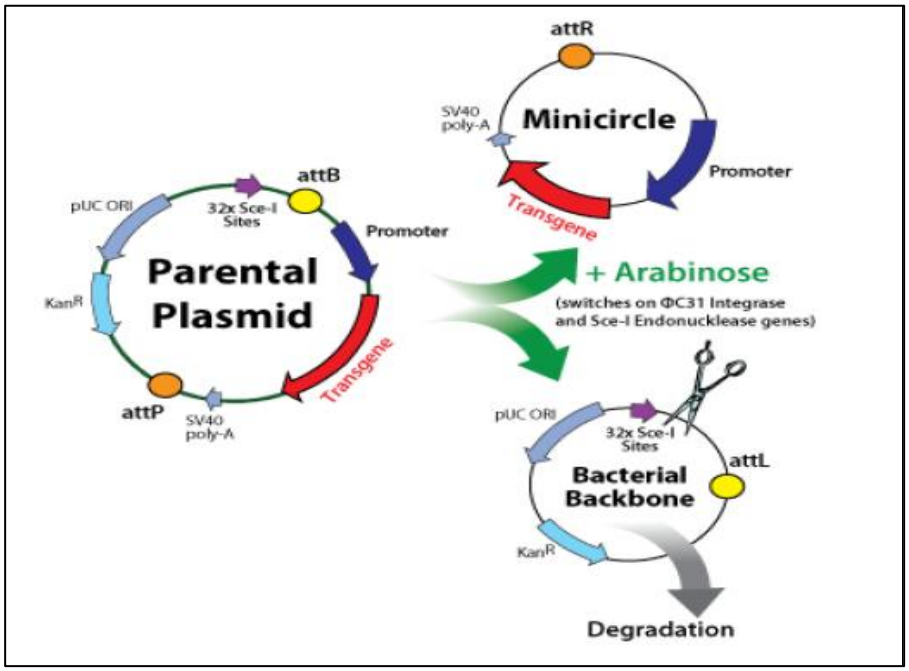

Supplementary Figure 2: Schematic representation of Minicircle induction procedure developed by System Biosciences.

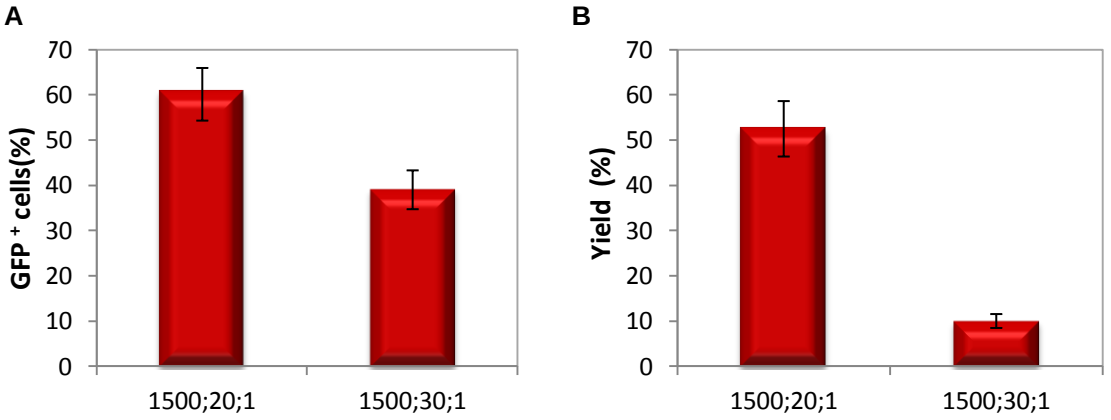

Supplementary Figure 3: Comparison of transfection efficiencies of CGR8-NSCs resuspended in RB and microporated using 1500V/20ms/1p and 1500V/30ms/1p as microporation parameters.

CGR8-NSCs were transfected with 1 µg of pVAX-eGFP and analyzed 24h after microporation; **A)** Percentage of GFP expressing cells was assessed by flow cytometry and **B)** Yield of Transfection was assessed by trypan blue exclusion method and flow cytometry. NM cells were used as controls (Control viability ≈92%, not shown) and the results are expressed as mean ± SEM of two independent experiments.

Supplementary Table 1: Percentage of CpG motifs in each DNA vector

	Size (bp)	No. CpG motifs (bp)	% CpG motifs
MC-GFP	2257	129	5.7
pCMV-GFP	3487	230	6.6
pVAX-eGFP	3697	248	6.7

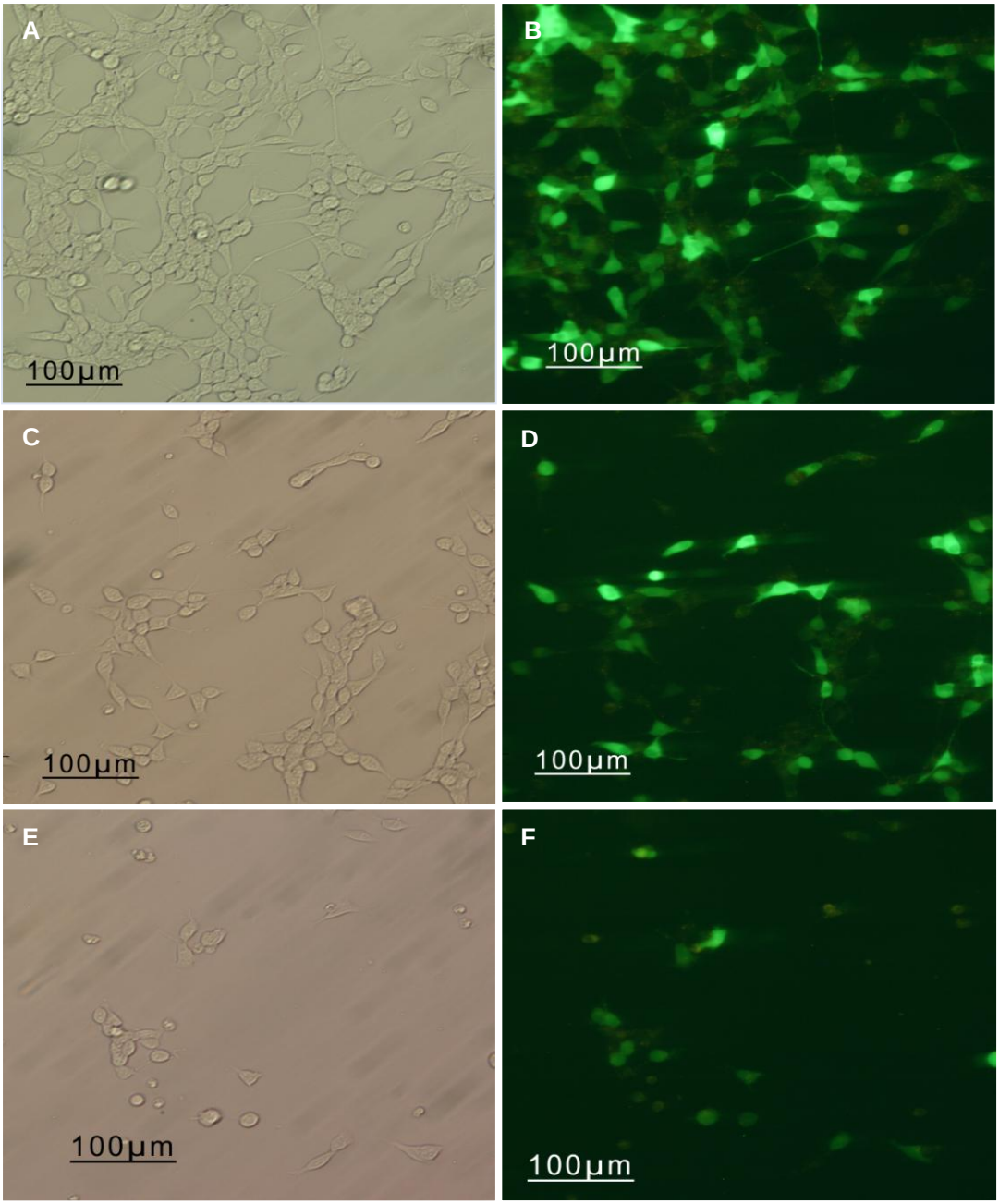

Supplementary Figure 4: Phase contrast (left) and fluorescence (right) microscopic view of transfected CGR8-NS cells.

CGR8-NSCs were ressuspended in RB and transfected with 2.0 x 10^{11} molecules of DNA vector. Images (100x) were obtained after 24h for CGR8-NS cells transfected with **A,B)** MC-GFP, **C,D)** pCMV-GFP and **E,F)** pVAX-eGFP.